D2.1 - Designs and specifications of an OWC able to integrate the negative spring

DATE: January 2016

PROJECT COORDINATOR:

WavEC Offshore Renewables

GRANT AGREEMENT NR: 641334

PROJECT: WETFEET

The WETFEET – Wave Energy Transition to Future by Evolution of Engineering and Technology project has received funding from the European Union's Horizon 2020 programme under grant agreement No 641334.

Report with one or more designs and specifications of an OWC able to integrate the negative spring; enhanced added-mass; survivability submergence and dielectric generators			
Project	WETFEET – Wave Energy Transition to Future by Evolution of Engineering and Technology		
WP No.	2	WP Title	System description
Deliverable No.	2.1		
Nature (R: *Report*, P: *Prototype*, O: *Other*)	R		
Dissemination level (PU, PP, RE, CO)	PU		
Lead beneficiary:	WavEC Offshore Renewables		
Contributing partners	IST, INNOSEA, SSSA		
Authors List:	Boris Teillant (WavEC) Yannick Debruyne (WavEC) António Sarmento (WavEC) Teresa Simas (WavEC) Marta Silva (WavEC) Rui Gomes (IST) João Henriques (IST) Maxime Philippe (INNOSEA) Adrien Combourieu (INNOSEA) Marco Fontana (SSSA)		
Quality reviewer	Teamwork & IST		
Status (F: final; D: draft; RD: revised draft):	F		
Due Delivery Date:	31/01/2016		
Actual Delivery Date:	29/01/2016		

Version no.	Dates and comments
0	22-Nov-2015 Deliverable structure defined
1	09-Dec-2015 Full draft of chapters 1 & 2
2	23-Dec-2015 Partial draft of chapters 3 & 4 and reviewed chapters 1 & 2
3	18-Jan-2016 Full draft
4	25-Jan-2016 Quality review on the full draft
5	29-Jan-2016 Document revised according to quality review – final version ready for submission

TABLE OF CONTENTS

TABLE OF FIGURES

TABLE OF TABLES

Executive Summary

This report presents Deliverable 2.1 of the WETFEET H2020 project – Report with one or more designs and specifications of an OWC able to integrate the negative spring; enhanced added-mass; survivability submergence and dielectric generators. It consists of an introductory description of the integration of the proposed breakthroughs into the OWC spar buoy along with a preliminary design analysis of the device.

After an initial system description of the OWC spar buoy without breakthrough features, each proposed breakthrough concept is presented. The working principle of the breakthrough ideas is accompanied with a scientific or technical justification highlighting their step-change potentials with respect to a "classic" OWC spar buoy as it has been explored to-date in the literature.

Additionally, further considerations on the OWC spar buoy are included in this report, namely:

- Marine operation strategies to allow the load-out, transportation, installation and retrieval of the OWC spar buoy,
- Preliminary design and structural analysis to identify the key structural requirements for the reference case of the OWC spar buoy (without featuring the breakthroughs)
- Potential environmental and cost impacts introduced by the breakthrough features

The deliverable concludes with a path toward the realization of the necessary studies to assess more precisely the potential impacts associated with each of the breakthrough. This numerical work will feed deliverable 2.3 and other work packages which are focusing specifically on some of the breakthroughs.

List of Acronyms

AEP	Annual Energy Production
CAPEX	Capital Expenditures
DE	Dielectric Elastomers
DEG	Dielectric Elastomer Generator (to refer to the whole generator)
EAM	Enhanced Added-Mass
EIA	Environmental Impact Assessment
FEM	Finite Element Method
FLS	Fatigue Limit State
IRR	Internal Rate of Return
LCOE	Levelized Cost of Electricity
NPV	Net Present Value
NS	Negative Spring
OPEX	Operational Expenditures
OWC	Oscillating Water Column
PTO	Power Take-Off
TRL	Technology Readiness Level
TPL	Technology Performance Level
WEC	Wave Energy Converter
WP	Work Package

1. INTRODUCTION

1.1. Context and motivation

Within the framework of the WETFEET H2020 EU funded project, a set of breakthroughs have been identified to address the obstacles that have been delaying the path towards commercialization of the wave energy sector. These breakthroughs are applied to two wave concepts, the OWC spar-buoy and the Symphony, under development by members of the consortium.

Work Package (WP) 2 of the WETFEET project serves as a technical base over which the development of the breakthroughs can be constructed. In this context, this initial report is intended to verify whether the proposed breakthroughs for the OWC spar buoy can be properly implemented. For this purpose, a global preliminary analysis of the OWC was conducted with three major objectives:

- Define the OWC spar buoy system specifications
- Deploy a set of tools relevant to the analysis of the core engineering challenges associated with the OWC spar buoy
- Engage with the integration of the breakthroughs to the OWC spar buoy

1.2. State-of-the art of the OWC device type

Over the course of the past 35 years, many R&D programs have investigated wave energy with the objective to accelerate the commercialization and exploit the potential of this vast source of renewable energy. Although technical feasibility has been demonstrated for a number of concepts, the wave energy sector longs to witness evidence of the expected technological convergence. There still exists a large diversity of WEC designs and it remains unclear which one(s) is (are) the best positioned to make a significant contribution to the energy market.

Among the various wave energy concepts, OWC-WECs have received significant attention from the research community since the early studies on wave energy in the late 70s and early 80s. The basic working principle of an OWC consists of a surface piercing chamber with a submerged opening in which an oscillating air-water interface is subject to time-varying pressure due to the action of the incoming wave field.

There exist several literature survey papers related to research and development associated with OWC concepts [1]–[5]. The most recently published review article by Falcão and Henriques [5] classifies OWC devices into 5 types, namely:

- Fixed-structure OWCs
- Breakwater-integrated OWCs
- Floating-structure OWCs
- Floating-structure WECs with interior OWCs
- Multi OWC devices

Table 1-1 attempts to provide some general insight into the past and current status of each of the above five OWC types. One should note that some OWC devices may fall into more than one category. To date, there is a relative significant difference of Technology Readiness Level (TRL) between these OWC types ranging from proof of concept until pre-commercial prototypes.

Moreover, onshore and offshore OWC technologies are hardly comparable due to the contrast in the engineering challenges they have to face. While onshore device are either mounted on fixed structure or to a breakwater, nearshore and offshore OWC devices typically require a mooring system and a complete electrical transmission system to the shore. Being offshore allows the exploitation of resources with higher energetic potential.

TABLE 1-1 INSIGHT ON THE FIVE OWC TYPES DEFINED BY FALCÃO ET AL.[5]

OWC type	TRL range	Examples of device development	Key advantages	Key disadvantages
Fixed-structure OWCs	4-7	Islay prototype, Pico plant, LIMPET, …	Accessibility Survivability Grid distance	Limited resource Visual impact Shore noise emission
Breakwater-integrated OWCs	4-7	Sakata plant, Mutriku plant, Civitavecchia plant, …	Accessibility Survivability Shared infrastructure Grid distance	Limited resource Design constraints Shore noise emission
Floating-structure OWCs	3-5	OE buoy, OceanLinx Mk3, Mighty Whale, OWC spar buoy, …	Offshore resource Visual impact	Accessibility O&M Grid distance
Floating-structure WECs with interior OWCs	2-3	U-Gen, Crowley et al. [6], Kurniawan et al. [7], …	Offshore resource Visual impact Enclosed PTO	Accessibility O&M Grid distance
Multi OWC devices	2-4	Seabreath, LEANCON, V-shaped 32 OWCs …	Modularity Scalability Power quality	Accessibility O&M Control

1.3. Contribution of the OWC spar-buoy device to WETFEET objectives

Pioneer researchers of wave energy had already investigated the concept of an axisymmetric floating OWC, sometimes called OWC spar buoy [8]–[10]. More recently, a report commissioned by the British Department of Trade & Industry [11] indicated that OWC spar buoy is considered the lower risk and most economic buoy among three OWC floating configurations.

In the WETFEET project, it is expected to build upon some recent optimization studies carried out by members of the consortium [12]–[14]. More specifically, breakthroughs ideas will be the subject of initial engineering analysis to assess their potential for cost-reductions. In a report by Sandia National Laboratory [15], several pathways for cost-reductions of OWC were identified. Among these pathways, one can associate the breakthroughs that will be the object of a preliminary study in the present report:

- Improved power conversion: both the Dielectric Elastomer Generators (DEG) and the tetra-radial turbine aim at enhancing the power conversion chain
- Optimized structural design and device profile: implementing the Negative Spring (NS), the Enhanced Added-Mass (EAM) and the survivability submergence will result in a more efficient and resilient structural design
- Array optimization: shared moorings through rigid and non-rigid connections are intended to have an overall positive impact on the cost of electricity
- Increased system reliability: submergence under harsh environmental conditions as well as DEG endeavour to improve the overall lifecycle reliability

While bottom-fixed, breakwater and floating ducted OWC device types have been largely investigated, there is arguably less published work on the OWC spar buoy. The low TRL of the OWC spar buoy (i.e. in the range 2-3) adduces the implementation of innovative and step-changing concepts leading to lower cost of electricity while demanding affordable R&D effort.

2. OWC SYSTEM DESCRIPTION

2.1. Main components

The OWC spar buoy consists of a cylindrical floater pierced by a hollow cylinder opened at the bottom to the sea water and the top to the pneumatic chamber. As presented in [12], a cross-sectional view of the OWC spar buoy is given in Figure 2-1. One can enumerate the key elements of submerged part of the device as:

- ➔ 6 cylindrical (1, 3, 6, 8, 10 and 11), 4 conical (2, 4, 5 and 9) and one toroidal (7) surfaces which can be divided into three main parts:
  - the floater – (surfaces 1, 2 and 11),
  - the small thickness tube (STT) – (surface 3) and
  - the large thickness tube (LTT) – (surfaces 4, 5, 6, 7, 8, 9 and 10)

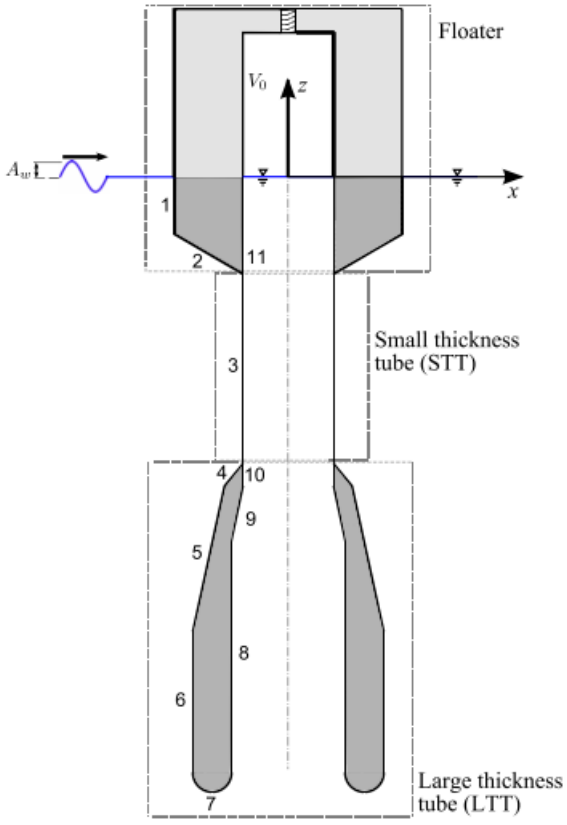

FIGURE 2-1 CROSS-SECTION VIEW OF A TYPICAL DESIGN FOR THE OWC SPAR-BUOY

2.2.Operating principle and energy conversion chain

The operating principle of an OWC resides in the cycle of compression-decompression of trapped air to flow through a turbine coupled to a generator. Unlike fixed OWCs, a floating OWC oscillates which leads to radiation of waves. With the proper structural design and control system, these oscillations are expected to enhance the power extraction efficiency from the incoming wave field. In terms of practical implementation, an air turbine must be connected to the OWC air chamber by some sort of ducting arrangement which must be then coupled to the generator. In order to optimise the efficiency of an air turbine one should achieve minimal interference between the generator and the air flow exiting the system.

Several air turbines to equip the OWC spar buoy have been considered in Falcão et al. [14] including a single and several multi-stages Wells turbine as well as a bi-radial impulse turbine. While it was found that the bi-radial turbine exhibits the best overall device production performance, further studies should be carried out to reflect more realistically some non-linearities and control strategies.

In a high-level energy conversion chain model, one can introduce the following three incremental steps:

1. Mechanical wave power: it corresponds to the resource power available in the incoming wave field interacting with the OWC spar-buoy
2. Pneumatic power in the water column: part of the incoming wave power induces a vertical motion in the water column which is converted into pneumatic power by the compression/expansion of the air enclosed in the inner chamber of the OWC spar buoy
3. Mechanical turbine power: the time-varying pressure inside the chamber drives a mechanical air turbine connected to the exterior atmosphere
4. Electrical power: part of the turbine shaft power can be converted into electricity by coupling it to a generator and the power electronics which can ultimately feed the grid

This process can be schematically represented as shown in Figure 2-2. It should be noted that this conversion chain only applies to the case of air turbines. DEG offer a more direct conversion principle which will be depicted in section 3.

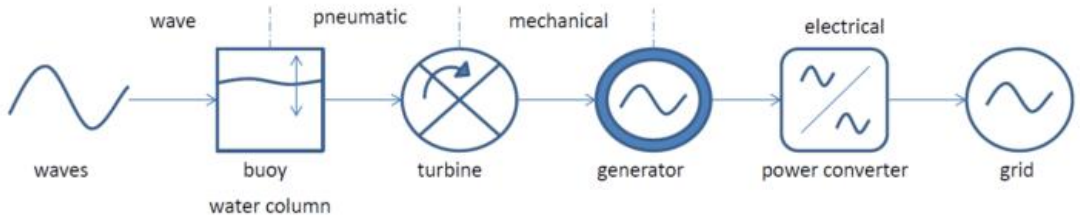

FIGURE 2-2 POWER CONVERSION CHAIN OF A FLOATING OWC WITH AN AIR TURBINE

2.3.Control mechanisms

To date, control systems for wave energy have been primarily developed with the objective of maximizing the power absorption or, more recently, maximizing directly the generated electrical power output of the devices. In the context of OWCs, control mechanisms have been predominantly implemented by means of valves which can regulate the level of air flow to drive the air turbine. Two valves are typically employed [2]:

- Relief valve: mounted in parallel with the turbine and connects the chamber with the outside atmosphere with the purpose of avoiding turbine stall for very large flow rates.
- High-speed stop valve: installed in series with the turbine to lock the air flow with the purpose of latching control or controlling the flow rate.

In practice, the majority of control law algorithm cannot circumvent the need for short-term wave forecasting. The wave prediction requirements essentially concern the need to inform the controller with values of free surface elevations or wave excitation forces. Such requirement originates from the non-causality of the optimal PTO force [16]. A recent comparative study of two methods for short-term wave forecasting at the Pico plant [17], shows that sensors measuring the free surface elevation up-wave of the plant and also the wave elevation inside the chamber are necessary for accurate estimations. Other auxiliary equipment commonly used for control mechanisms include a data acquisition system, power electronics and a servo-computer.

Concerning the OWC spar buoy, Henriques et al. [18] tested a simple generator control law both numerically and experimentally using a dry test rig. Relief valve and high-speed stop valve have also been considered to control the threshold limits of the generator rotational speed. Future work should seek a solution to cope with the large pressure difference observed between the pneumatic chamber and the atmosphere.

2.4.Mooring system

The OWC spar buoy device uses a slack-mooring system with three equally-spaced mooring lines, connecting the buoy to the sea bottom, as shown in Figure 2-3 from a top view perspective. The mooring line configuration experimentally tested at Plymouth university's wave tank for a scaled version of a 16 meter diameter buoy at 80 meter water depth is presented in Figure 2-4 [19].

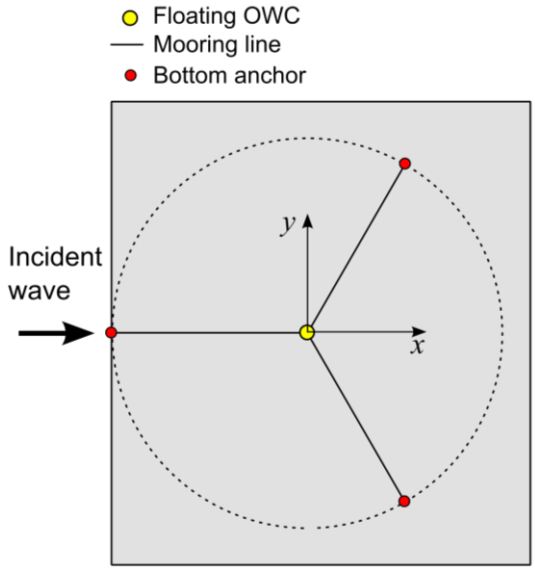

FIGURE 2-3 TOP VIEW OF A SLACK MOORING SYSTEM WITH THREE BOTTOM MOORED LINES OF AN ISOLATED OWC SPAR BUOY

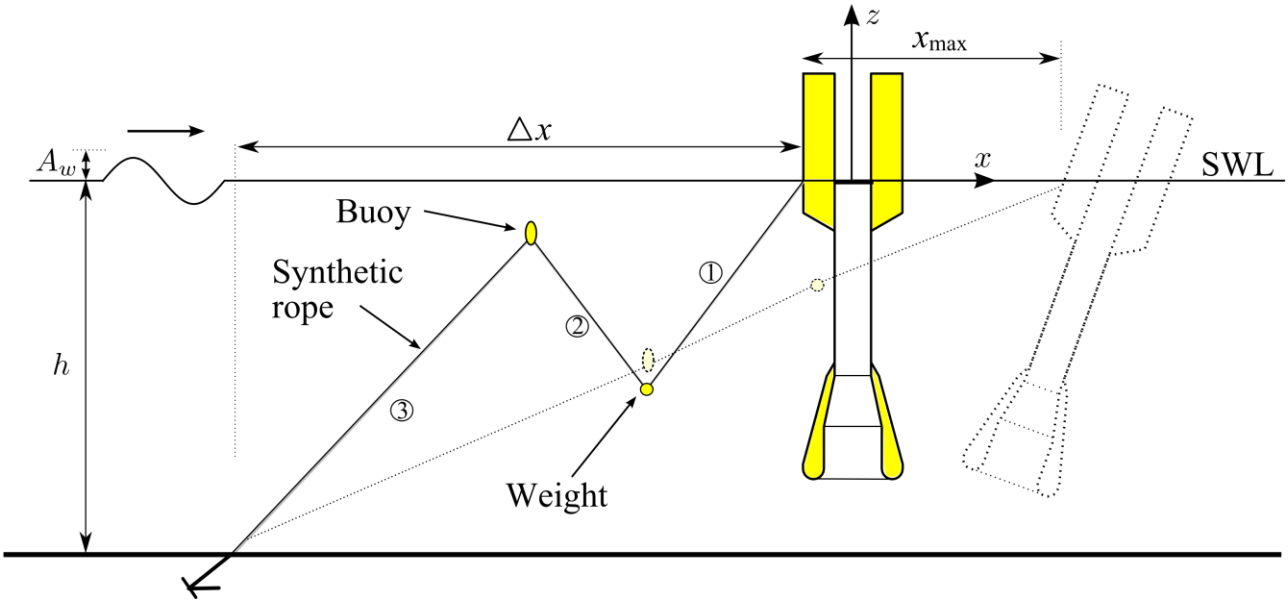

FIGURE 2-4 REPRESENTATION OF A SINGLE LINE OF THE SLACK-MOORING SYSTEM. THE EXTREME SITUATION WITH FULLY STRETCHED MOORING CONFIGURATION IS REPRESENTED IN DOTTED LINES

Under extreme wave conditions, it was observed that the mooring system of Figure 2-4 can become fully stretched (situation represented in dotted line), which results in abnormal mooring loads. This occurs for the mooring line closer to the wave source when it is oriented with the wave direction, as presented in Figure 2-4.

For this reason, an upgraded version of the slack-mooring type is suggested, where instead of connecting the third line directly to the bottom anchor, the line is connected to a light studded chain, which is partially suspended above the bottom floor as depicted in Figure 2-5. The addition of a heavy studded chain laid on the sea floor and anchored to the bottom is also proposed. Under extreme line tension, the heavy chain becomes suspended above the sea floor increasing largely the stiffness of the mooring system. The three-section line cables that connect the device, small floater and buoy could be synthetic ropes. This upgraded version of the slack-mooring type will be the object of a load assessment calculation in chapter 5 in order to confirm the expected benefit of this new mooring design under extreme conditions.

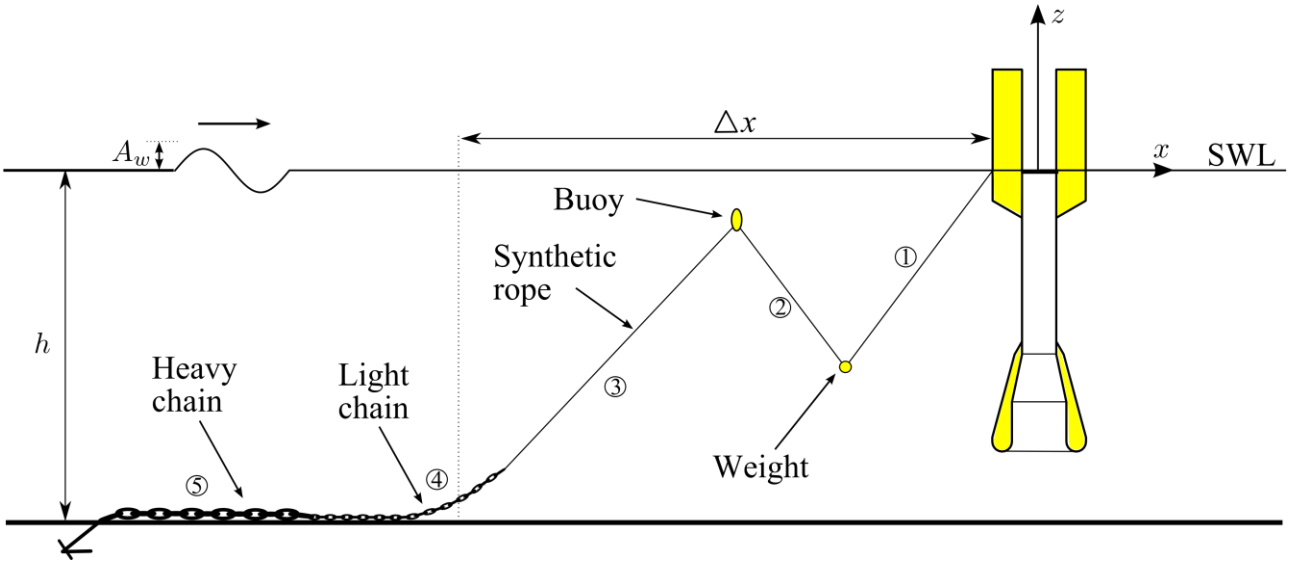

FIGURE 2-5 UPDATED VERSION OF THE SLACK-MOORING SYSTEM WITH TWO ADDITIONAL SECTIONS OF STUDDED CHAIN

3. INTEGRATION OF BREAKTHROUGHS

This chapter comprises the core elements serving as basis for the implementation of the breakthroughs into the OWC spar-buoy. For each of the four breakthroughs previously identified (NS, EAM, submergence and DEG), the following initial considerations will be made:

- Technical description of the concepts with scientific background,
- Highlighting the breakthrough potential of the concept for wave energy applications,
- Proposing suitable and relevant architectures on how to integrate the breakthrough concepts into the OWC spar-buoy,
- Reviewing the existing numerical models to analyze the breakthroughs and
- Strategy for developing (and/or coupling) the relevant numerical tools that are currently missing or incomplete to carry out the relevant engineering analysis and performance assessment

Preliminary high level considerations for two other breakthroughs (tetra-radial air turbine and shared moorings) are included although there will receive dedicated treatment in other work packages of the WETFEET project.

3.1. Negative spring

The OWC spar buoy can be considered as a heaving point absorber WEC because:

- The horizontal dimensions (e.g. buoy diameter) are much smaller than the typical wavelength of fully-developed seas.
- The body structure and internal free surface of the water column are primarily moving in heave.

The OWC spar buoy operates by using the relative heaving motion between the internal water free surface and buoy structure. Each of these has its natural frequency which should be sufficiently apart for the device to be efficient in a wide frequency range. To achieve optimal power absorption conditions from a hydrodynamic standpoint, it has been shown that one should aim to bring the heaving point absorber in resonance with the incoming waves [20], [21]. However, this requires having buoys with large dimensions and mass. This results from the usually large hydrostatic spring associated with heaving devices. A way to circumvent this is to use a negative spring mechanism to compensate the very strong hydrostatic spring-like effect, therefore resulting in a smaller and less stiff device.

Under a sinusoidal wave excitation with frequency ω and amplitude A_w and under the linear potential flow theory, the complex amplitude Z of the body heaving oscillation is given by:

$$Z = \frac{A_w \Gamma}{[G + K_{ext} - \omega^2(m + A)] - i\omega(B + B_{ext})} \quad \textbf{(3-1)}$$

Where Γ is excitation force coefficient (in N/m) that only depends on the frequency of the incident wave (and not on the body oscillation), B is the hydrodynamic radiation damping of the body (in N.s/m), A and m are the hydrodynamic added mass and the body mass (both in kg), respectively, B_{ext} represents an external damping (in N.s/m, produced by any external power take-off equipment and/or by viscous dissipation), K_{ext} represents an external spring (in N/m, due to the power take-off equipment, the mooring lines, or any other process or mechanism) and G is the hydrostatic stiffness coefficient (in N/m) of the body.

The mathematical problem described in Eq. (3-1) corresponds to a "classic" mass-spring-damper physical system for which the natural angular frequency ω_0 (in rad/s) can be readily determined as:

$$\omega_0 = \sqrt{\frac{G + K_{ext}}{m + A}} \quad \textbf{(3-2)}$$

Theoretically, the maximum mean power $P_{a_{max}}$ (in W) of a single mode WEC can be achieved under the following condition [22]:

$$P_{a_{max}} = \frac{|\widehat{F_e}|^2}{8R} \quad \textbf{(3-3)}$$

Where:

- $\widehat{F_e}$ is the complex excitation force due to the incoming waves (amplitude in N, phase in rad)
- R is the hydrodynamic reactance of the body which relates to the total damping of the system $B + B_{ext}$ (in N.s/m)

From Eq. (3-3), the optimal velocity amplitude $\hat{u}_{opt}$ (in m/s) of the WEC in this mode of absorption can be derived:

$$\hat{u}_{opt} = \frac{\widehat{F_e}}{2R} \quad \textbf{(3-4)}$$

To achieve the optimum power absorption conditions enunciated in Eq. (3-3) or (3-4), there exist (at least) two alternatives entirely equivalent:

- Phase and amplitude control which forces the oscillation velocity to be in phase with the excitation force and also that the velocity amplitude satisfies Eq. (3-4),

- Reactive control or complex-conjugate control which essentially consists of cancelling the inherent reactance of the system through a PTO reactance compensation.

While the above two control strategies have been the object of intense R&D effort over the past three decades (see the review article by Ringwood et al. [16]), sub-optimal power absorption conditions have also been investigated more recently. Moreover, it can be shown that, from a PTO mechanism perspective, power absorption maximization leads to the following conditions on the PTO stiffness, K_{PTO}, and the PTO damping, B_{PTO}:

$$K_{PTO} = \omega^2(m + A) - G - K_{mor} \quad \textbf{(3-5)}$$

$$B_{PTO} = R \quad \textbf{(3-6)}$$

where K_{mor} is the mooring stiffness coefficient (in N/m)

In the case of heaving point absorber like the smaller designs of the OWC spar buoy, the hydrodynamic stiffness G is the dominant term in Eq. (3-5) (as long as the diameter of the buoy remains relatively small, i.e below 12 meters) which means that K_{PTO} has to be negative for optimum control. To counterbalance this term with the objective to approach optimal power absorption conditions, it emanates that the external spring K_{ext} (which includes the terms K_{PTO} and K_{mor}) can be devised to approach or deviate from the resonance frequency (see Eq. (3-2)), depending on the objectives of the design and application.

Negative springs (NS) are mechanical concepts which aim at improving the performance of resonant WECs by tuning K_{ext} (usually by acting on K_{PTO}) over a wider range of incoming wave frequencies than just the natural frequency of the structure. By nature, NS are unstable systems when deviated from their equilibrium position. This property is key to reducing the stiffness of heaving point absorber WECs and thus significantly improving the energy density performance (e.g. ratios of annual energy production per unit of mass, per unit area or per unit of PTO force).

Concepts exploiting the NS effects are currently under development by some researchers and technology developers. In particular, the WaveSpring patented technology [23] which is part of the CorPower wave energy device has been the object of several studies over recent years [24], [25]. The WaveSpring provides phase control by a NS mechanical arrangement that inherently widens the response bandwidth of point absorbers without the need for real-time wave information or prediction algorithms.

In the case of the CorPower point absorber device, the NS module acts directly on the linear mechanism of the buoy. This avoids the losses associated with transmitting large reciprocating energy flows through the PTO system, a challenge that has limited the practical use of phase control methods known as reactive control. Experimental wave tank testing of a 1:16 scaled CorPower device [25] featuring pressurized cylinders to simulate the NS arrangement have shown promising results, in particular:

- Three times higher ratio of absorbed energy to significant PTO force.
- Mooring line forces with maximum values less than 2.5 times the mean tension

Another experiment conducted at the wave basin of Aalborg university tested a single rotor of the WEPTOS pitching WEC device with two different NS setups [26]. While no conclusive performance improvement was noticeable from the physical model testing campaign (probably due to frictional losses), a simple numerical model indicates positive benefits in terms of efficiency of the device over a broader wave spectrum compared to the configuration without NS.

Also recently, Zhang and Yang [27] developed a wave-to-wire numerical time domain model capable of simulating the effects of non-linear snap through PTO mechanisms which resemble very much the WaveSpring concept proposed for the CorPower device. Zhang and Yang [27], [28] demonstrated that negative spring effects have the potential to increase the power capture performance of heaving point absorbers in both regular and irregular waves. Further insight regarding the impact of the relative difference between the natural frequency of the body and the incoming wave frequency is given. The effects of the PTO damping coefficient and the significant wave height on the power capture performance of the negative spring concept are similar to those of the linear WEC.

Unlike the mechanical spring arrangement proposed by others, alternative NS concepts will be investigated for the OWC spar buoy. Instead of controlling the PTO mechanism, these alternative methods directly act on the hydrodynamic properties of the device. In the project, two negative spring methods that use hydrostatic effects associated with the shape of the OWC spar structure, will be explored to produce a negative spring effect without requiring any mechanical or electrical component. This is expected to increase the level of reliability of the system as problems associated with the fatigue of mechanical or pneumatic springs are avoided. These two NS methods can be used in other heaving point absorbers but the extension to other heaving devices other than OWC will not be undertaken in WETFEET.

The first NS method is intrinsically non-linear and as such requires non-linear numerical modelling. An in-house partially non-linear code will be used at WavEC to study this effect. This non-linear time-domain code computes the Froude-Krylov and hydrostatic forces [29], [30] taking into consideration the actual position of the body and water free-surface, instead of their mean position. To further improve the realism of the numerical simulations the most promising configurations will be analysed with a fully non-linear Computational Fluid Dynamic (CFD) tool [31]. This modelling approach will allow improving the understanding of viscous effects (including vortex shedding) both in the water column flow and external flow.

The second NS method on the other hand is intrinsically linear and will be studied with linear wave models in the frequency and time domains. If time allows it, CFD will be used to assess viscous effects.

The work to be undertaken will address the impact of the two negative spring methods on the device performance and motions and also on the stability of the device. For each OWC

geometry a parametric analysis will be taken to understand the effect of the main relevant geometrical parameters.

3.2. Enhanced added-mass

An intrinsic geometric characteristic of the OWC spar buoy is the addition of a submerged mass which allows for the enhancement of the added mass. The primary aim of this so-called Enhanced Added Mass (EAM) is to reduce the device natural frequency in order to tune it in accordance to the frequency of the predominant incoming waves while preserving the hydrostatic stability.

One of the benefit of choosing an enlarged submerged shape (with concentrated added mass) at the bottom of a spar floating structure is essentially to avoid having a structure with a substantially longer draft which would be potentially more expensive and not suitable for shallow to intermediate water depth. There exist a few different ways of increasing the added mass (flat plates, horizontal cylinders, spherical ballast, etc); however, structural constraints should be accounted for when designing the submerged structure.

Moreover, the submerged mass should preferably be located deep enough in order to reduce the interference with the optimized radiation characteristics of the floater (which is essential to maximize power absorption in the case of WECs). Therefore, the added mass coefficient of the submerged mass should be roughly frequency independent (and so equal to the infinite-frequency added mass coefficient).

In [12], Gomes et al. optimize simultaneously 5 design parameter variables of the OWC spar buoy in terms of average annual power available to the turbine, denoted, $\bar{P}_{ann}$. The length l_3 and the thickness t_3 of the submerged mass along with the internal diameter at the bottom of the OWC spar buoy d_3 are part of these 5 design variables (see red circles in Figure 3-1). The distance between the floater and the submerged mass l_2 and the internal diameter of the spar buoy d_2 are the other two optimization design variables (see black circles in Figure 3-1). Although it is difficult to conclude on the most favourable size for the submerged mass based on the results from [12], some valuable insight can be retrieved, including:

- The submerged mass should be placed deep enough to avoid radiative effects with negative impact on $\bar{P}_{ann}$(confirmation of the previous statement)
- There exist a region where the relative values of d_3 and t_3 lead to optimal $\bar{P}_{ann}$

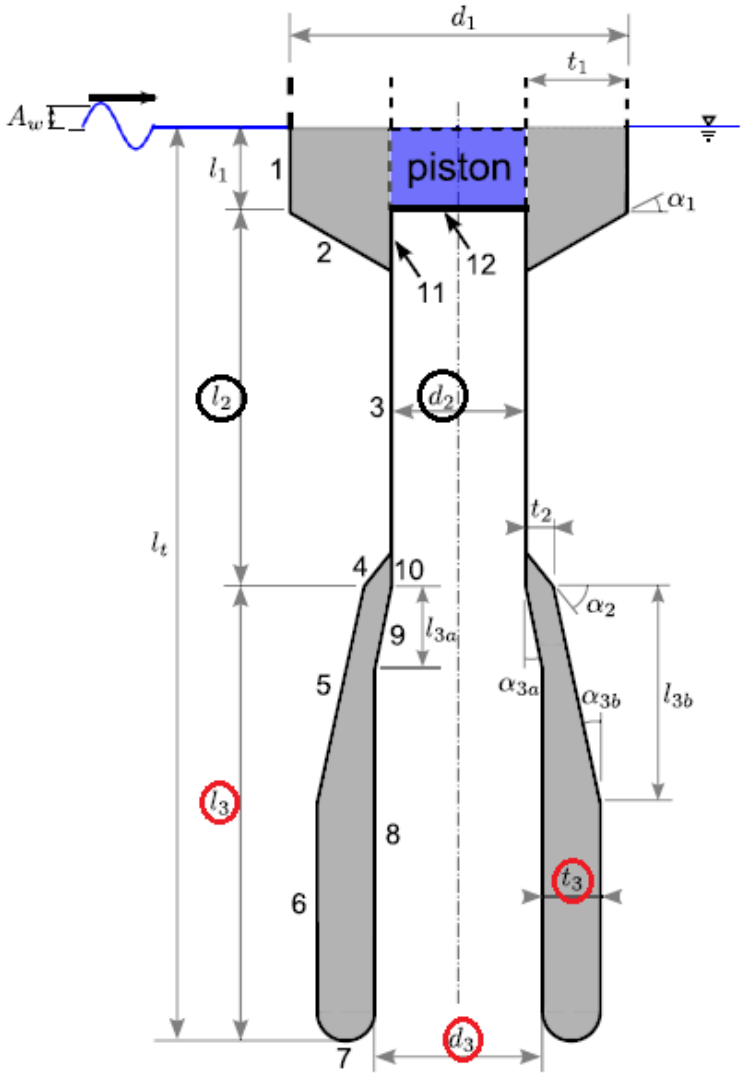

FIGURE 3-1 OPTIMIZATION VARIABLES CONSIDERED IN [12]: THE SUBMERGED MASS PARAMETERS ARE CIRCLED IN RED

Eventually, the submerged mass also contributes to lowering the gravity centre and so contributing to the vertical stability of the device. In chapter 5, the preliminary design and structural analysis will consider reference design cases of the OWC spar buoy already featuring the EAM following the design optimization results previously obtained in [12]. This will allow understanding better the stresses that the structure can experience under extreme load cases.

Future work to investigate further the optimal shape of the submerged mass could consist of adding a stability criteria to the optimization scheme proposed in [12], which would have to consider a detailed mass distribution. Replacing the objective function $\bar{P}_{ann}$ to account for the added cost incurred by the construction of such submerged mass is also a possibility.

3.3.Survivability submergence

The majority of floating WECs, such as the OWC spar buoy, are moored on the surface of the ocean and - as a result - are fully exposed to storms. This is one of the major causes for the conspicuous survivability issues affecting wave energy technology (and any surface-floating structure in the ocean, for that matter).

Given the utmost importance of survivability in the relatively high upfront capital cost of WEC prototypes deployed offshore, device developers often preferred a retrieval strategy in anticipation of harsh environmental conditions for floating WEC prototypes during sea-trials. However, in the context of a commercial array of multi-unit devices, it seems economically hardly acceptable to rely on the need to hire vessel(s) every time the forecast indicates rough climate conditions which may damage the devices.

To overcome this issue, one solution is to design the device and its structure in such a way that they can sustain the vast majority of environmental conditions observed at site. This implies applying large safety factors in the structural design process. Finding the appropriate trade-off between safety, cost and performance of the device can thus become a highly complex equation. Alternatively, devising an on-site survivability strategy allowing the protection of the device during harsh environmental conditions, which would not require the intervention of specialized vessel/equipment/personnel, appears to be an attractive solution. For this reason, device submergence is proposed as a breakthrough concept in the WETFEET project.

Device submergence under extreme conditions is expected to increase survivability and reduce the structural requirements of mooring lines and possibly of device structure and components, thus allowing for fewer materials to be used. There are three critical aspects to consider from a hydrodynamic engineering perspective:

- hydrostatic pressure increase due to converter submergence,
- the submergence level for significant wave load reduction under storm conditions and
- the stability of the converter in the water column, as well as the solutions for water tightness

Concerning the OWC spar buoy, it is envisaged to achieve device submergence by:

- actively controlling the mooring elements so that a pulling force towards the sea-bottom is applied to the fairleads of the device
- ballasting the structure to increase the submerged mass of the body
- a combination of the two previous methods

The combination of these submergence methods is schematically represented in Figure 3-2.

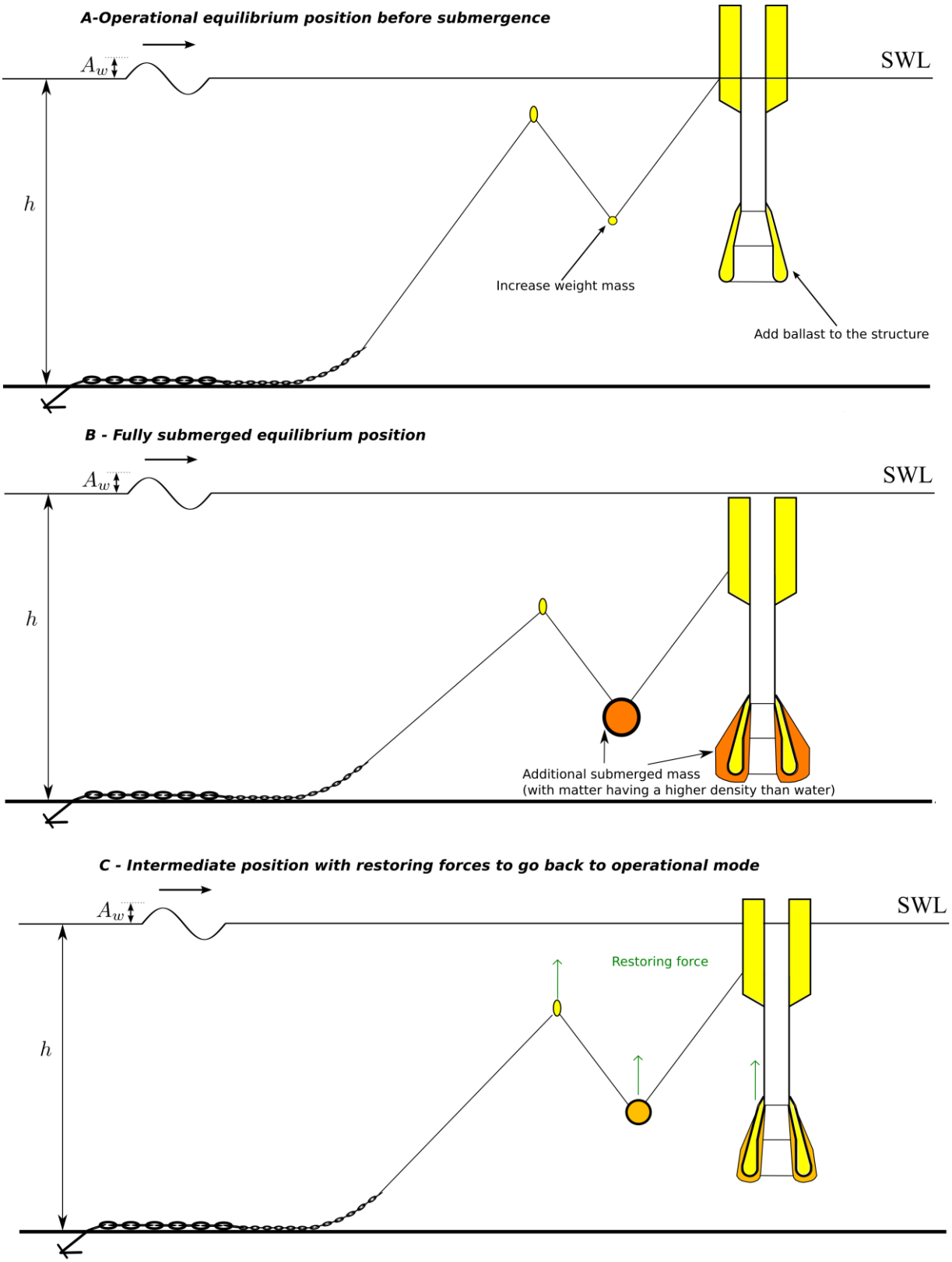

FIGURE 3-2 SUBMERGENCE STRATEGY FOR SURVIVABILITY: FROM OPERATIONAL EQUILIBRIUM POSITION (ON TOP) TO THE FULLY SUBMERGED POSITION (CENTRE) AND THE RECOVERY OF THE SUBMERGED BODY TO OPERATIONAL MODE VIA RESTORING FORCES (BOTTOM)

The feasibility of the proposed submergence strategies will be assessed through various stages of numerical modelling. First, a frequency domain analysis will be used to quantify the wave-induced motions of the device (particularly in heave, pitch and roll) at different submergence depth. For this purpose, the hydrodynamic coefficients of the OWC spar buoy structure will be computed using the WAMIT boundary element method code. Frequency domain Response Amplitude Operators (RAOs) can then be plotted to verify the viability of the wave-induced motions.

To complement the above simplified linear study, the non-linear time domain code Ship@Sea is going to be utilized. Ship@Sea is based on the strip theory [32] and was originally designed to simulate the parametric rolling of a vessel. For the purpose of this study, the code is going to be extended and adapted to the OWC spar buoy. As for the frequency domain calculations in WAMIT, several draft levels of the OWC spar buoys will be investigated. Time domain motion responses of the OWC spar buoy will result from this analysis. Together, the two above-mentioned studies will help de-risking the submergence strategy by assessing the susceptibility and severity of occurrence of dynamic instabilities in waves of the OWC spar buoy during the procedure.

Furthermore, the complete behaviour of the submerged device as well as the solicitation of the mooring lines in storm conditions will be assessed through the Orcaflex™ software. Orcaflex™ is one the most recognized tools to model the dynamics of ships and offshore cables such as mooring lines or power cables. On the one hand, static analysis can provide a quick and accurate numerical assessment of the forces required to submerge and emerge (restoring forces) the OWC spar buoy (this work shall be conducted as part of WP3 of the WETFEET project). On the other hand, time-domain simulations of the fully submerged configuration (see centred Figure 3-2-B) under extreme wave conditions shall provide further insight on the design requirements for the OWC spar buoy. Finally, physical model testing will also be carried out in the FloWave tank facility in Edinburgh to assess experimentally the submergence procedure.

The expected results from these simulations will be compared to the reference case studied in chapter 5 to assess the additional structural and design requirements associated with the submergence of the entire device. In turn, this numerical modelling work will support the feasibility study, the in-depth engineering analysis and the tank testing which will be carried out in work package 3.

Other critical engineering issues associated with the submergence strategy which shall be discussed include:

- Ensure proper sealing and protection of all on-board electro-mechanic and power electronic equipment fitted in the OWC spar buoy
- Risk of collision with the seabed
- Material corrosion, and in particular, the areas of the structure alternatively exposed to the atmosphere or the ocean/sea environment

- Fatigue of the critical active parts of the submergence procedure

3.4. Dielectric elastomer generators

The operating principle of a Dielectric Elastomer Generator (DEG) has been conceived less than a decade ago and it is based on a solid-state deformable transducer made of elastic polymers that can convert mechanical energy into direct electricity via the variable-capacitance electrostatic generation principle.

In the context of wave energy harvesting, potential advantages of DEG technology over traditional PTO systems are: direct drive cyclical operation with good energetic efficiency that is almost independent of wave period; easier installation and maintenance; and lower costs.

The feasibility of energy conversion from waves to electricity employing a DEG-PTO has been generally demonstrated in the Future Emerging Technologies EU Project PolyWEC (Pj.Ref. 309139). Specifically, DEGs have been tested in operative condition in scaled laboratory experiments and show their concrete potentiality as energy converters. Small scale prototypes in the watt-range have shown experimentally verified wave-to-wire energy densities of 0.7 kJ/kg (i.e. energy converted for each cycle by a unit volume of employed dielectric material) and conversion efficiencies of nearly 25%, but the concrete perspective is to increase energy density up 1 kJ/kg and efficiency up to 60-70% in a relative short timeframe by using more efficient materials. For example, the multinational company WACKER Polymers has recently released a new product that is specifically dedicated to the application of DEG named Elastosil Film that is showing extremely promising performances.

However, given that, DEGs are still an emerging technology, they have not yet been considered for prototypes in the framework of WETFEET project, but the further development of DEG as future PTO is pursued in a dedicated work package, WP5. Specifically, the main aim of WP5 is to: 1) conceive and characterize new conducting and dielectric deformable materials (beyond the sole silicone elastomers investigated within the PolyWEC project) that will be pursued to enhance DEG performances; 2) as well as to validate their fatigue life and degradation; 3) develop and verify more accurate models that will be employed for the design and control of the system.

However, in order to steer the research toward tangible applications, a study is going to be conducted in order to define DEG-PTO to be integrated into the concrete WEC concepts of spar-buoy OWC and Symphony. An accurate definition of the layout and dimensioning of a possible DEG-PTO to be integrated in such WEC concepts should go through an in-depth hydrodynamic analysis that is not yet available at the current stage of the project. However, it is possible to draw an initial hypothesis of layout through a preliminary analysis based on theoretical considerations and on the results of previous experiments conducted by some of the partners of the consortium. Specifically, the following approach is assumed:

- Converted energy density: the amount of energy that can be converted by a unit of mass of dielectric elastomer is limited by a set of known boundary conditions such as maximum deformation of the material (in operational conditions) and maximum electrical filed that the dielectric can hold. This means that for a given energy output we can foresee a minimum requirement for the volume of needed materials.
- Power matching at specific frequency: in order to have a preliminary dimensioning of the mass/volume of dielectric material that is needed it is necessary to specify the peak power of the device and the typical working wave period that is assumed.
- Considerations on manufacturing and deployment: based on general consideration on manufacturing, transportation and installation an initial layout can be defined.

Figure 3-1 presents the scheme of such approach. Once the peak power is decided, it is possible to estimate the minimum quantity of material that has to be employed to guarantee that such peak power target is reached.

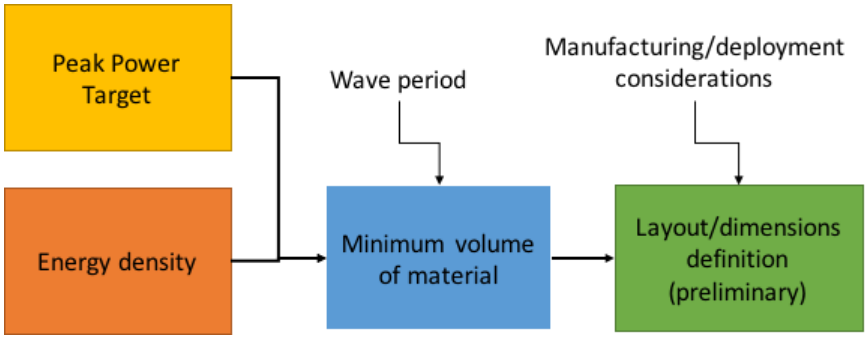

FIGURE 3-3 SCHEME OF THE APPROACH FOR THE PRELIMINARY LAYOUT AND DIMENSIONING OF THE DIELECTRIC ELASTOMER GENERATOR DEG FOR THE OWC SPAR BUOY

Concerning the OWC spar buoy it is foreseen to study three different geometries that features three different power scales. Table 3-1 provides, for the three different geometries, the prospected ratings of nominal power (P_n) and peak power (P_{pT}) of a suitable air turbine coupled with the different WECs.

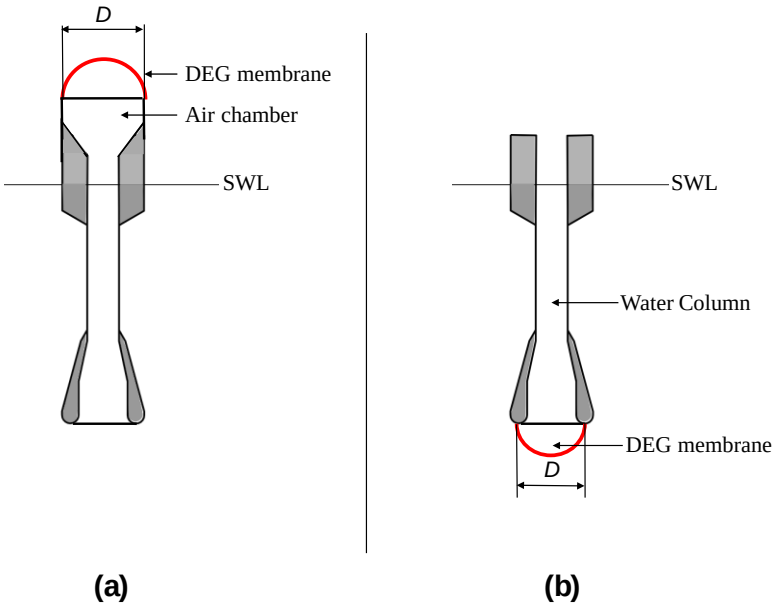

FIGURE 3-4 SCHEMATIC REPRESENTATIONS OF TWO POSSIBLE SOLUTIONS FOR THE INSTALLATION OF THE DIELECTRIC ELASTOMER GENERATOR FOR THE OWC SPAR BUOY

Given the expected peak power rates of the turbines it is possible to provide a preliminary dimensioning of the DEG defining the minimum volume of dielectric material that is required. Specifically, assuming an energy density of the DEG of 0.7kJ/kg and a wave period of 10s we obtain the following required volume of materials for the 3-meter, 6-meter and 12-meter diameter OWC spar buoys: Ω_3=171kg; Ω_6=928kg, Ω_{12}=3571kg[1].

At first instance, the architecture of the Circular-Diaphragm DEG (CD-DEG) is adopted, in which the deformation of the DEG is obtained through the inflation of a relatively thin membrane made of alternative layers of conductive and dielectric elastomers (see Figure 3-2a). In this configuration, the air acts as a compliant reactive component between the water mass and the DEG which might worsen/influence the dynamic response of the WEC. In a further version, in order to eliminate the volume of air, architectures where the membrane is submerged could be considered (Figure 3-2b). In both these architectures, assuming that the diameter of the membrane is equal to the buoy diameter, the approximate thickness (s) for the DEG membrane can be calculated (see Table 3-1) for the DEG.

TABLE 3-1 DIMENSION AND DATA OF HYPOTHETIC TURBINE PTO AND PEAK-EQUIVALENT DEG-PTO

Geometry	***Diameter***	***Turbine Data***		***DEG-PTO Data***		
		P_n	P_{pT}	P_{pD}	Ω	s

[1] Such relevant amount of material should be considered a major limitation to the technology since it is relevant to remark the raw material can feature a very low-cost of approximately 1-2€/kg.

3-meter	3 m	4 kW	12 kW	12.37 kW	171 kg	25 mm
6-meter	6 m	23 kW	65 kW	65.31 kW	928 kg	33 mm
12-meter	12 m	101 kW	250 kW	253.3 kW	3571 kg	32 mm

3.4.1. Manufacturing considerations

Industrial manufacturing of large DEGs is still a rather unexplored challenge. The simplest and cheapest manufacturing process that is foreseen to be employed for achieving a multilayer structure of conductive and dielectric layers is the multi-roll-coating technique. This process is a continuous production process that applies coating during the rolling process of the raw material.

However, due limitation in the length of the rolling cylinder of rolling machines the maximum dimensions of membranes than can be processed are limited. Specifically, it is estimated that with current production technologies it is foreseen the possibility of manufacturing membranes with a maximum diameter of 4m. In order to overcome this limitation new roll-coating machines or different production processes have to be studied.

A different arrangement of membranes could be conceived according to this constraint by considering the use of multiple 4-meter membranes for the two larger OWC spar buoy geometries. Specifically, Table 3-2 indicates the number of 4-meter membranes that should be required for the 6-meter and 12-meter geometries. These are calculated assuming that the maximum thickness of the multilayer membrane should be below 35 mm in order to limit the number of layers.

TABLE 3-2 NUMBER OF 4-METERS MEMBRANE REQUIRE TO PROVIDE THE EQUIVALENT PEAK-POWER

Geometry	**n. of 4-m**	P_{pk}	**Peak Power**
6-meter	3	25.mm	65.9kW
12-meter	9	32mm	253.3kW

3.5. Preliminary considerations for shared moorings

As for the offshore wind sector, if offshore wave energy is to become commercially viable, farms of multi-unit devices will be deployed at a given site rather than single unit in order to be able to payback (through the revenue generated by the electricity produced) the significant upfront capital cost notably due to the electrical grid connection. Due to the relatively low rated power of full-scale wave energy machines that have been tested to-date (typically less than 1 MW), it is anticipated that a large number of WEC units would be needed to match the

300-500MW offshore wind farms which are now close to be competitive with other renewable energy plants.

In the preliminary mooring design proposed for the OWC spar buoy (see Table 5-2 based on the upgraded mooring design), the total length of each mooring line element for one unit can be calculated as shown in Table 3-3. Obviously, if dozens or even hundreds of units are to be deployed, the procurement and installation cost associated with such considerable length of moorings and the number of anchors would represent a significant share of the cost of electricity and possibly jeopardize the economic viability of the project.

Mooring design parameter	Total value for one OWC spar buoy unit
Total length of mooring line (line 1 + line 2 + line 3) [m]	674.75 = 3*(142.45+42.45+46.65)
Total length of light chain [m]	96
Total length of heavy chain [m]	150

TABLE 3-3 TOTAL LENGTH OF MOORING LINE ELEMENT FOR ONE OWC SPAR BUOY UNIT

One possible response to this challenge is the share of mooring lines and anchoring points between neighbouring devices. In the WP6 of the WETFEET project, both non-rigid connections and rigid-connections strategies will be studied. Researchers from the Instituto Superior Técnico (IST) [33] have recently performed a battery of tank tests with various mooring configurations of the OWC spar buoy. In particular, they compared the motion response and the mooring loads of a single OWC spar buoy with an array of three OWC spar buoys with shared anchoring points and inter non rigid connections as presented in Figure 3-5.

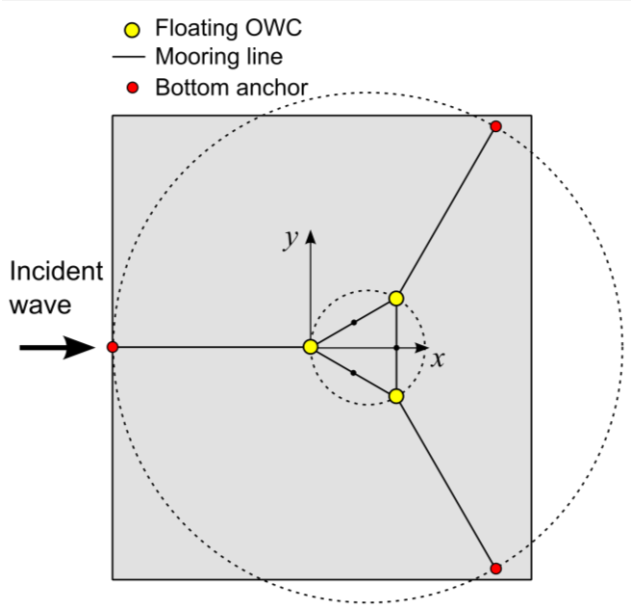

FIGURE 3-5 SCHEMATIC TOP-VIEW OF AN ARRAY OF THREE OWC SPAR BUOYS WITH SHARED MOORING LINES AND ANCHORING POINTS

Within the framework of WP6, the objective will be to build upon the key lessons learnt during this campaign of tank tests while proposing alternative mooring configurations in an array of OWC spar buoys. Both numerical and experimental modelling will be carried out to support this task. Examples of rigid or non-rigid connections configurations in a pentagon-shaped cluster of 5 OWC spar buoys are schematically represented in Figure 3-6.

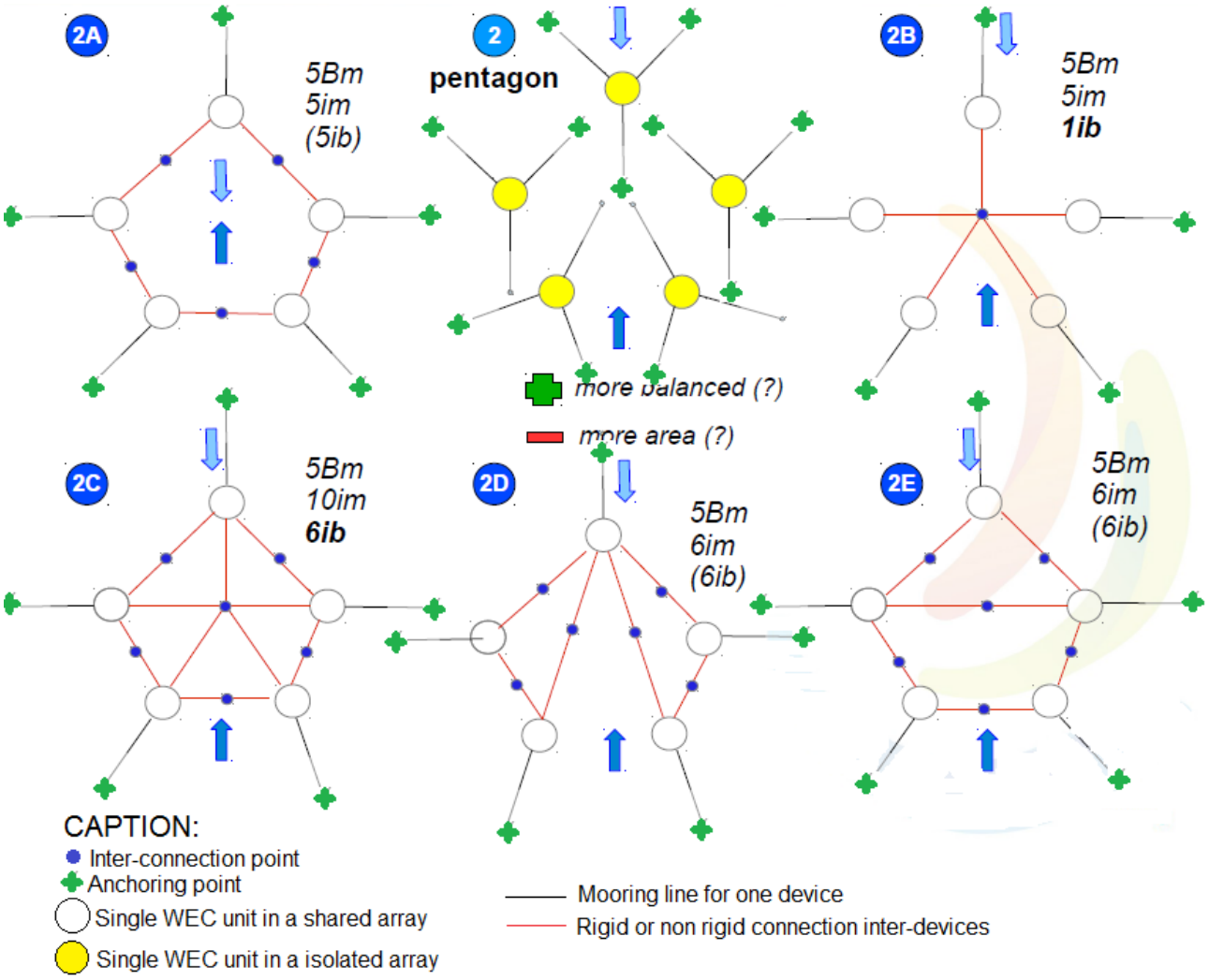

FIGURE 3-6 CONCEPTUAL TOP VIEW OF A PENTAGON-SHAPED ARRAY OF 5 OWC SPAR BUOYS WITH RIGID OR NON-RIGID CONNECTIONS

3.6. Preliminary considerations for the tetra-radial air turbines

The new tetra-radial turbine has two sets of rotor blades mounted on a common shaft and axially offset from each other. Each set of rotor blades is complemented by a set of guide vanes, as in a conventional unidirectional turbine. This whole set of rotor blades and guide vanes may be regarded as forming two conventional single-stage radial turbines, T_1 and T_2, see Figure 3-7 and Figure 3-8.

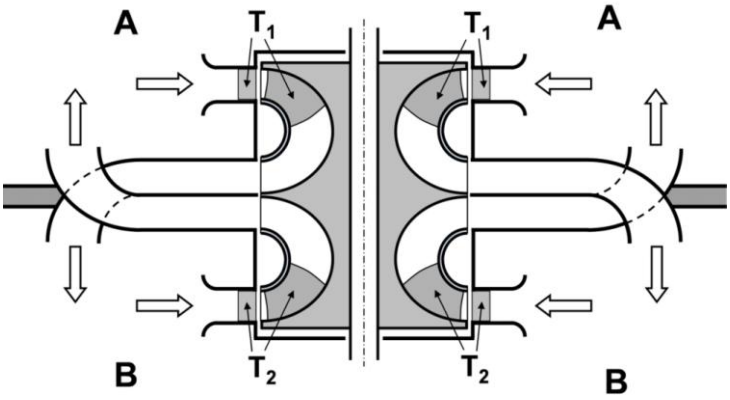

FIGURE 3-7 NEW TURBINE WITH RADIAL-FLOW ROTOR CONFIGURATION

The turbine operates between spaces A and B at pressures p_A and p_B, respectively. These spaces are the OWC air chamber and the atmosphere. When $p_A > p_B$, the air should flow only through blade-set T_1. Conversely, when $p_A < p_B$, the air should flow only through blade-set T_2. This is made possible by a double set of curved ducts arranged circumferentially and alternately open to space A and space B, as represented in Figure 3-7, and, in perspective, in Figure 3-9. Each rotor is connected to the corresponding set of curved ducts by a bladeless space bounded by curved and plane walls of revolution, as shown in Figure 3-9. The radial extent of this bladeless space allows it to act as a diffuser, recovering part of the kinetic energy at rotor exit before flow entrance into the curved-duct manifold. The tetraradial name comes from the two inlets and two outlets resulting from the twin turbine rotor configuration

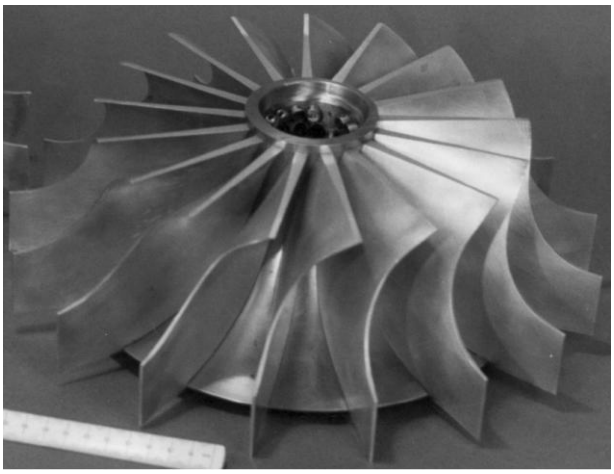

FIGURE 3-8 THE RADIAL-FLOW TURBINE ROTOR

The configuration of the new turbine makes it possible to install an axially-sliding cylindrical valve that is operated to prevent air from flowing in the reverse direction, see **Erro! A origem**

da referência não foi encontrada. This is made easier by the relatively small size and stroke of the valve. The valve actuator may be pneumatic, electrical or of other type. The valve may be used in three positions as represented in Figure 3-10. If the valve actuator is fast enough (opening and closing times not exceeding a few tens of a second), then this provides a way of phase-controlling the OWC plant by latching. Latching is known to be an effective way of substantially increasing the amount of energy absorbed from the waves by oscillating body devices. Only recently, with the emergence of new turbines like the biradial turbine, has phase control by latching started to be seriously considered as applicable to OWC converters [34], [35]. This could be enhanced by the new turbine proposed here.

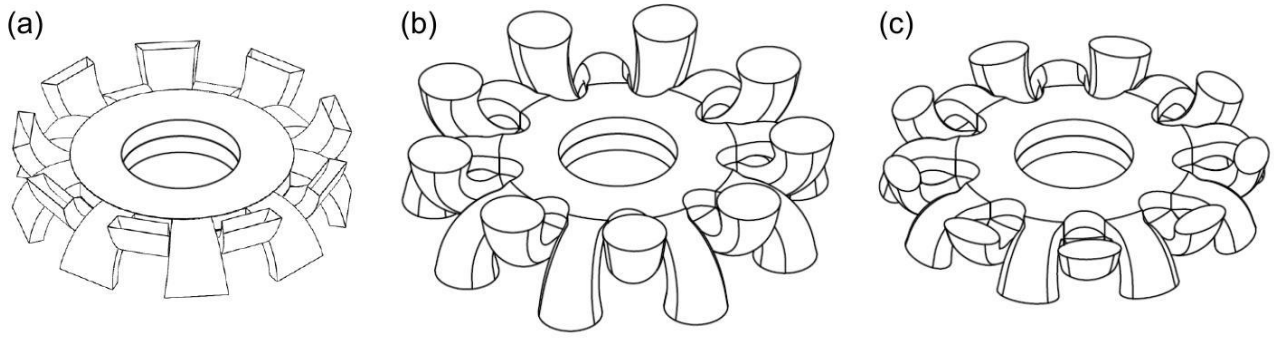

FIGURE 3-9 PERSPECTIVE REPRESENTATION OF THE CURVED-DUCT MANIFOLD, WITH A) TRAPEZOIDAL, B) CIRCULAR AND C) ELLIPTICAL EXIT SECTIONS

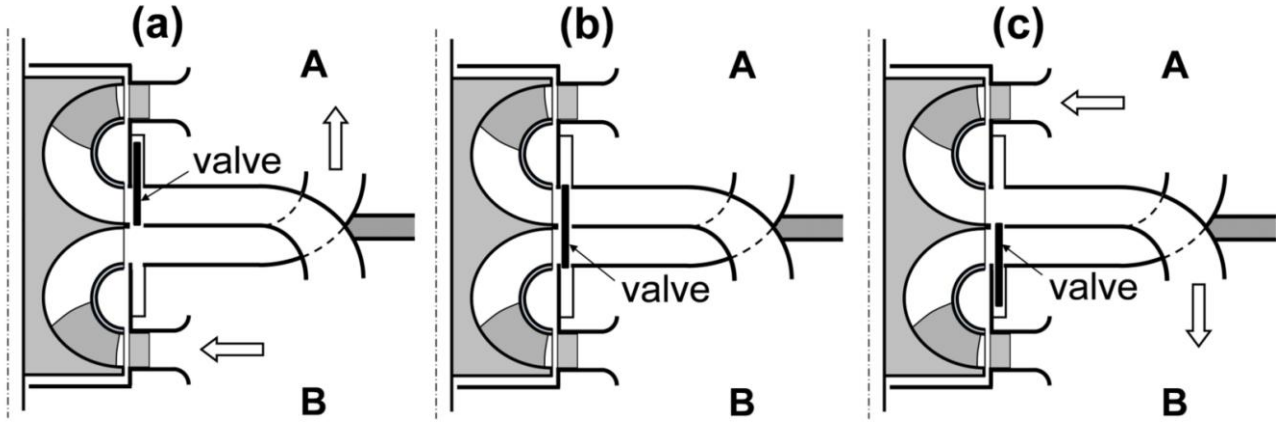

FIGURE 3-10 THREE-POSITION AXIALLY-SLIDING VALVE

The efficiency of the self-rectifying axial-flow impulse turbine with fixed guide vanes is severely affected by the losses at the entry to the downstream row of guide vanes. Peak efficiencies measured in model testing do not exceed about 50% (as compared with about 75% for the most efficient Wells turbines), see Fig. 3.13. On the other hand, the efficiency curves do not exhibit the sharp drop typical of most Wells turbines. The performance of the axial-flow impulse turbine can improve by about 10 to 15% if moveable guide vanes are used

instead of fixed ones. However, the mechanical complexity of this solution has deterred its use. The so-called biradial turbine [36], is a radial impulse turbine that is symmetrical with respect to a plane perpendicular to its axis of rotation. The flow into, and out of, the rotor is radial. The rotor is surrounded by a pair of radial-flow guide-vane rows; each row being connected to the corresponding rotor inlet/outlet by a duct whose walls are flat discs. In one of the versions of the biradial turbine, the guide vane rows may be removed from, or inserted into, the flow space by axially displacing the whole guide vane set, so that the downstream guide vanes are prevented from obstructing the flow coming out of the rotor. In this version, the measured peak efficiency of a turbine model was about 79%, possibly the highest efficiency of a self-rectifying air turbine measured so far. The fixed guide vane version of the biradial turbine suffers from losses at the entry of the downstream row of guide vanes. The curved-duct manifold configuration of the tetraradial removes the downstream row of guide vanes allowing the use of a very efficient rotor that does need to be symmetric as the case of the other turbines. Peak efficiencies of about 86% have been numerically predicted [37].

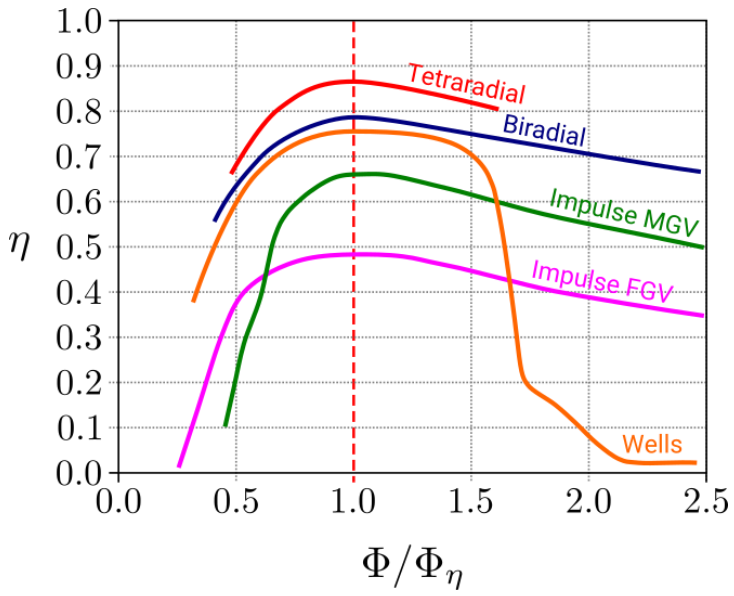

FIGURE 3-11 EFFICIENCY COMPARISON BETWEEN THE RADIAL ROTOR TETRARADIAL TURBINE, THE BIRADIAL TURBINE, THE AXIAL IMPULSE TURBINES WITH MOVEABLE GUIDE VANES (MGV) AND FIXED GUIDE VANES (FGV) AND THE WELLS TURBINE.

4. MARINE OPERATIONS

Maritime operations requirements are expected to present an important influence in the design considerations of the OWC spar buoy. Five distinct operations strategies are envisaged: load-out at the shipyard, transportation to the deployment site, installation, retrieval and access for maintenance. The oil and gas industry has a large experience in marine operations with spar structures. However, some operations involve complex and expensive procedures, e.g. the rental of specific vessels for transportation and installation or the offshore ballasting, which are avoided for the case of the OWC spar buoy. In fact, the cost of O&G offshore operations represents a significant part in the whole project. This relative cost becomes even more significant if the same know-how and infrastructure are applied in wave energy. The reduction of these costs through the simplification of processes and the use of fewer support infrastructures is a challenge that all wave energy technologies face.

The load-out scenario at the shipyard assumes that the OWC buoy spar structure, built mainly from steel plate, is assembled in its horizontal position. The structure is ballasted with concrete in the yard to reduce the complexity of the on-site installation. The design of the LTT has to take into consideration that the ballasting is performed with the spar lying down. All PTO equipment (turbine, generator, valves, etc.) is fitted in the OWC structure prior to the load-out operation and must be securely fastened. This also includes an auxiliary floater (airbag) attached inside the OWC tube with the objective of keeping the device in its horizontal position in water (not represented in the figure). The OWC spar-buoy is deployed in the ocean using a lifted load-out strategy with a land-based crane (e.g. a gantry crane or a tower crane). The structure is lifted using two points on the structure outer surface, near the bottom part, where the centre of gravity is located, as shown in Figure 4-1. The structure could then be deployed in the ocean for transportation. An alternative option that may also be considered is the application of a float-away load-out strategy, with the device being build, ballasted, and/or assembled (including the auxiliary floater) in a dry dock. After which the dry dock is flooded and the device floats in an approximate horizontal position due to the combined buoyancy of the device and auxiliary floater.

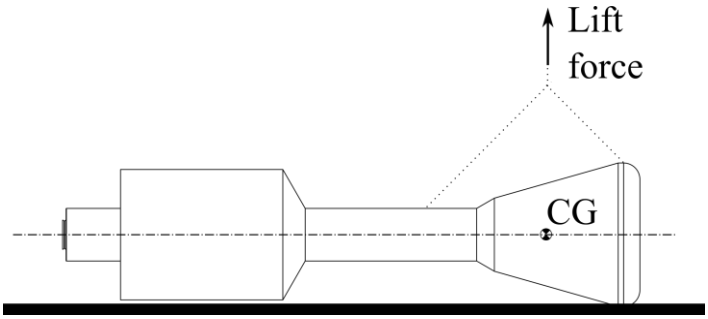

FIGURE 4-1 REPRESENTATION OF THE LIFT POINTS FOR THE LIFTED LOAD-OUT STRATEGY WITH THE BUOY HORIZONTAL

The transportation of the OWC spar buoy from the shipyard to the offshore deployment site is made in its horizontal position or with a small angle of inclination in order to guarantee the protection of sensitive equipment at the top of the floater (e.g. the air turbine and generator) from sea water impacts during transportation (an effect not expected to occur during normal operation and device submergence). The inclination angle selection should also take into account the drag effect importance during the transport. For this purpose, a large insufflated auxiliary floater (airbag) is attached to the structure, inside the OWC tube, to provide the additional buoyancy to keep the device horizontally stable, as shown in Figure 4-2. The auxiliary floater length extends to the exterior of the OWC tube due to the structure low centre of gravity. The exact dimensions of the auxiliary floater should be such that the floater buoyancy force cancels the natural righting moment of the spar structure. It may be necessary to design a non-axisymmetric floater or use additional floaters fixed outside the structure to avoid rotation about the axisymmetry axis. The top of the auxiliary floater is attached to the top of the structure to avoid contact with the turbine. The structure is then towed to the deployment location using one of more Anchor Handling Tug Supply (AHTS) vessels.

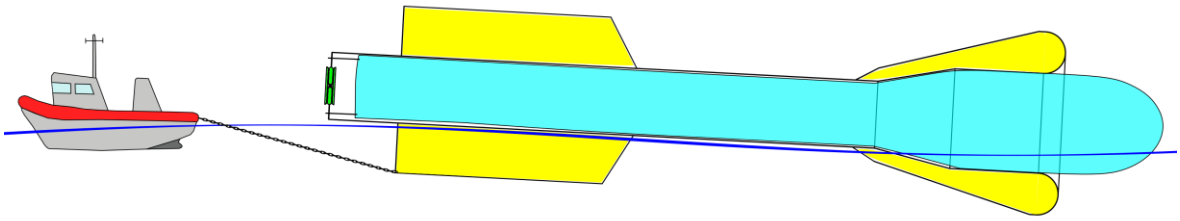

FIGURE 4-2 REPRESENTATION OF THE WET TRANSPORT OPERATION

The installation operation starts with the pre-lay of the mooring lines and installation of the anchors in the specified locations. This can be done prior to the transport of the OWC spar-buoy and with the same AHTS vessel. The type of anchor used for the deployment is dependent on the seabed profile. However, drag-embedment anchors may be an adequate selection for most applications if the following conditions are verified: a seabed slope smaller the 10°, a soft seafloor and the inexistence of nearby pipes and cables. For other conditions, suction caisson, gravity and pile anchors may be considered.

Installation of the OWC spar buoy proceeds placing the structure at the deployment location, keeping the connection with the AHTS vessel. Due to the need of dealing with an unmoored structure, this operation should be carried out under very low energetic sea states. The auxiliary floater is deflated in a controllable way through a valve connected to the OWC spar buoy air chamber, which as an open hatch to the exterior during the entire operation. If necessary, the auxiliary floater can be deflated using several independent sections to guarantee a sequential deflation. With the loss of buoyancy due to the deflation, the structure will recover stability by tending to the vertical position, as shown in Figure 4-3. After the structure reaches an upright position, the completely deflated auxiliary floater is extracted from the bottom part of the floater. Additional suction equipment may be necessary to complete the deflation.

Finally, the mooring cables are connected to the fairlead and tensioned to the specified pre-tension value. The electrical cable is then attached to the structure through a dry-mate connection and the air chamber is sealed. At this stage, the OWC spar buoy is ready for operation.

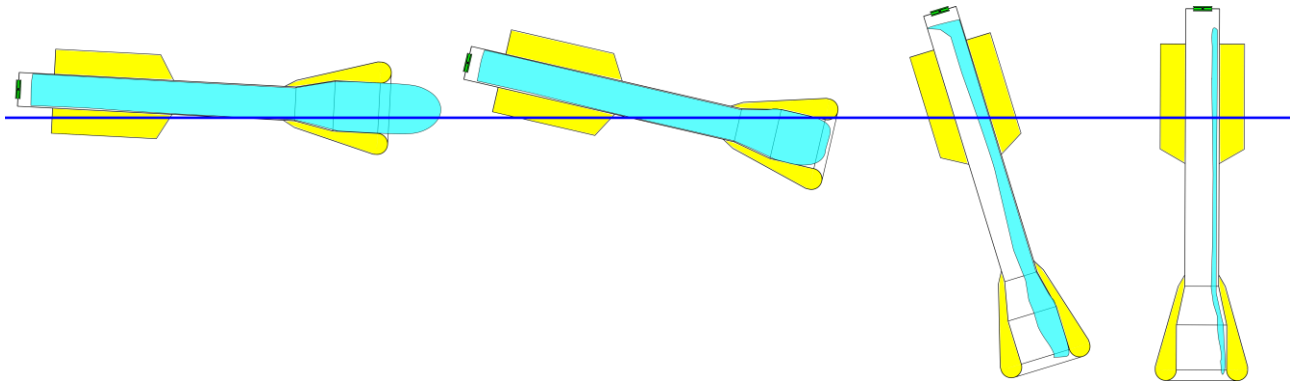

FIGURE 4-3 SCHEMATIC REPRESENTATION OF THE DEFLATION OF THE AUXILIARY FLOATER DURING THE INSTALLATION OF THE OWC SPAR BUOY

The retrieval of the OWC spar buoy is performed by reversing the installation method. The auxiliary floater placed inside the air chamber through a hatch and is attached to the top of the structure and released through the OWC tube, with a small weight at the end to keep it stretched. At this stage, a cable is connected to the AHTS vessel and the mooring lines are released from the fairleads, before a prior reduction of the line pre-tension. The auxiliary floater is inflated using a compressor on a vessel and the structure recovers its initial horizontal position. Water trapped inside the tube during inflation can flow through the open hatch. Since the structure is inclined during the retrieval operation, all equipment fitted inside the device must be securely fastened.

The access of individuals to the OWC spar buoy deck is done using a ladder fixed to the exterior surface of the cylindrical floater. Access to the top of the floater, where the turbine and generator are installed, is also made through a ladder. A small crane installed on the deck can be used for the recovery and delivery of equipment.

An alternative scenario to this set of operations may be considered for cost reduction if the construction yard is close to the deployment site (few kilometres) and if the construction yard has adequate bathymetry for the transportation of the spar structure in the vertical position, without the use of any auxiliary floating system. In this case, the load-out can be done through a lifted load-out or a float-away load-out strategy (if the dry dock has enough water depth when flooded). The device, initially in the horizontal position, will be in its vertical position when freely floating. An AHTS vessel is used to tow the structure to the deployment location. Due to the high drag forces induced on the structure, which depends on the towing velocity, the structure is likely to have a significant inclination angle while being towed. If this alternative scenario is considered, the load cases should be adapted.

Although the installation strategy is significantly different, a point of comparison with the OWC spar buoy in the marine renewable field is the Hywind. This concept, developed by Statoil (Norway), is a spar-type structure that supports a wind turbine. A Hywind full-scale prototype, a cylindrical spar with a draft of 100 m, was deployed off the coast of Norway in 2009 [38]. Its installation used a more conventional approach, being commissioned to Technip, a company with large experience in the oil and gas offshore industry. The spar structure was towed (about 1000 km) horizontally without ballast to sheltered waters near the deployment site. The floating structure was ballasted with water and rocks. An auxiliary vessel was fixed to the spar structure during the ballast, tower and turbine installation. The tower and turbine installation also required a floating crane. The complete prototype was later transported to the deployment location and fixed to three mooring lines. In that case, the complexity of the tower and turbine installation and the necessity of auxiliary vessels are likely to have influenced the selection of the spar structure installation. The method used was cost-intensive and Statoil launched a challenge to several companies in the marine sector to develop innovative ideas to simplify and reduce the installation [39]. The main focus of this challenge was the assembly efficiency of the tower and the turbine, considering the deployment of several devices.

5. PRELIMINARY DESIGN

The purpose of this chapter is to summarize the findings of computational results for the hydrodynamic and structural analysis of three geometries of the OWC spar buoy. The design of these three OWC spar buoy does not feature any breakthrough previously described apart from the EAM for which sufficient design optimization is already available. Results obtained for the three diameters chosen (respectively 3, 6 & 9 meters) will serve as a reference base scenario to make technical assessment in comparison with the OWC spar buoy implementing one of the breakthroughs.

5.1. Design specifications

Three geometries of the OWC spar buoy are considered for this preliminary design study as summarized in Table 5-1 below.

TABLE 5-1 SPECIFICATIONS OF THE THREE GEOMETRIES CONSIDERED FOR THE PRELIMINARY DESIGN STUDY

Reference	Diameter [m]	Draft [m]	Height [m]	Steel thickness [mm]	Centre of gravity [m]	Dry mass [t]
OWC Spar buoy 3x9	3	9	12	8	-6.69	36.83
OWC Spar buoy 6x18	6	18	26	12	-13.04	183.06
OWC Spar buoy 12x36	12	36	51	15	-28.62	1217.4

The station-keeping system detailed in Figure 2-5 is composed of 3 regularly and equally spaced lines to maintain the OWC spar buoy in an equilibrium position (i.e. two anchor form an angle of 120° with the centre of the OWC spar buoy). The mooring system was adjusted for each OWC so that the surge resonance period of the device is around 100 s. Details of the mooring system for the three type of OWCs can be found in Table 5-2.

TABLE 5-2 MOORING SPECIFICATIONS OF THE THREE GEOMETRIES CONSIDERED FOR THE PRELIMINARY DESIGN STUDY

Mooring properties	OWC Spar buoy 3x9	OWC Spar buoy 6x18	OWC Spar buoy 12x36
Horizontal length [m]	195.2		
Water depth [m]	60		
Weight dry mass [kg]	2562	10622	63252
Weight density [kg/m3]	5600		
Buoy dry mass [kg]	0.1		
Buoy density [kg/m3]	250		
Length of line 1 [m]	142.45		
Length of line 2 [m]	42.45		
Length of line 3 [m]	46.65		
Length of light chain 4 [m]	32		
Light chain diameter [mm]	20		
Light chain weight [N/m]	75		
Length of heavy chain 5 [m]	50		
Heavy chain diameter [mm]	60		
Heavy chain weight [N/m]	675		
Surge resonance period [s]	90	142	146

Table 5-3 gives the environmental load conditions considered for the preliminary design study. Data were extracted from various sources including the ONDATLAS to characterize the wave, wind and current conditions at the Leixões site off the West coast of Portugal. The regular design wave for the 100-year sea-state is obtained as follows [40]:

$$H_{max} = 1.86 * H_s$$

$$T_{min} = 11.1\sqrt{\frac{H_s}{g}}$$

$$T_{max} = 14.4\sqrt{\frac{H_s}{g}}$$

The current velocity considered for the design is 0.65 m/s. It is obtained as the sum of the wind generated current (0.4 m/s) and the tidal current (0.25 m/s).

TABLE 5-3 SUMMARY OF THE ENVIRONMENTAL LOAD CONDITIONS CONSIDERED FOR THE PRELIMINARY DESIGN

Parameter	Value
Location coordinates (Leixões)	41° 12.2' N, 9° 5.3 W
H_s - 100 year period [m]	14.8
T_e – 100 year period [s]	17.4
H_{max}* [m]	27.53
T_{min}* [s]	13.63
T_{max}* [s]	17.69
Current speed [m/s]	0.65

5.2.Structural loads

5.2.1. Wave induced loads

In this section, the methodology followed by WavEC to compute the wave pressure induced loads on the 3 geometries of OWC spar buoy is detailed. At this stage, it is supposed that the OWC spar buoy is vertically standing still in the water, at equilibrium position.

A WAMIT® model of the OWCs was built using the higher-order discretization method. The OWC spar buoy geometry is represented by an assembly of panel which size is small enough to ensure grid independency, so that the results converge and that they provide an accurate estimation of the hydrodynamic loads per vertical slices (see Table 5-4).

TABLE 5-4: MAXIMUM PANEL SIZE IN WAMIT™

Buoy geometry	3 m diameter	6 m diameter	12 m diameter
Maximum panel area (m^2)	0.0028	0.0246	0.1142

At first approach, it is considered that the OWC spar buoy is a 1D hollow beam that extends along the vertical z axis (pointing upward). The slices were defined such that their upper and lower limits coincide with the limits of the panels defined by WAMIT (to avoid partial contributions from some panels to some slices which is difficult to quantify). Analytical development of the method to calculate the wave-induced loads in the required format for the structural analysis is given in appendix 7.A.

In order to realize a first structural assessment of the OWC spar buoys, the 3D components of the forces induced by the hydrodynamic pressure on vertical slices (of height lower than 0.5 m) along the column when a regular wave passes were computed. It is supposed that the OWC is fixed, and therefore the 'radiation' component of the dynamic pressure is neglected. This radiation pressure should however be included in more refined studies.

The theory behind the calculation of those loadings is detailed in section A. In particular, the use of dipole panels to model the central column is explained. It can be seen on Figure 5-1 that the real part of the diffraction pressure on the central column is much lower than on the rest

of the OWC spar buoy: indeed, dipole panel provide the user with the pressure jump across the panel, which in this case is significantly lower than the actual pressure applied on the outer surface of the column.

The properties of the regular wave equivalent to the 100-yr storm were detailed in section 5.1: H = H_{max} = 27.53 m and T = T_{max} = 17.69 s. A summary of the results is available in the appendices, in **Erro! A origem da referência não foi encontrada.**1, **Erro! A origem da referência não foi encontrada.**2 and **Erro! A origem da referência não foi encontrada.**C-3. Those results include the 3D components of the force issued from the integration of the complex diffraction pressure over each slice, as well as the real component of the hydrostatic force (integration of the hydrostatic pressure over each slice).

NB: According to the design basis, a safety factor of 1.3 is to be applied to those values when input to the beam model.

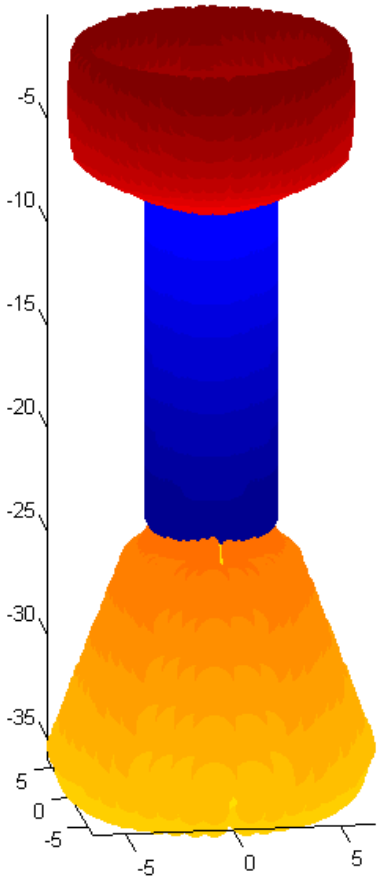

FIGURE 5-1 REAL PART OF THE DIFFRACTION PRESSURE CALCULATED BY WAMIT™ (H_{MAX},$T_{P,MAX}$)- 12 M DIAMETER OWC SPAR BUOY

5.2.2. Mooring loads

The methodology followed by WavEC to compute the mooring loads is detailed in this section.

In order to realize a proper structural design of the structure, the forces applied by the moorings on the OWC spar buoy structure at the fairlead connections should be assessed. It

was decided that those loads would be extracted from time-domain simulations realized through Orcaflex™. For this purpose, a set of ten 3-hour simulations in an irregular sea-state representative of the 100-year storm return period were realized for each OWC. The main numerical settings of Orcaflex for these simulations are detailed in the appendices.

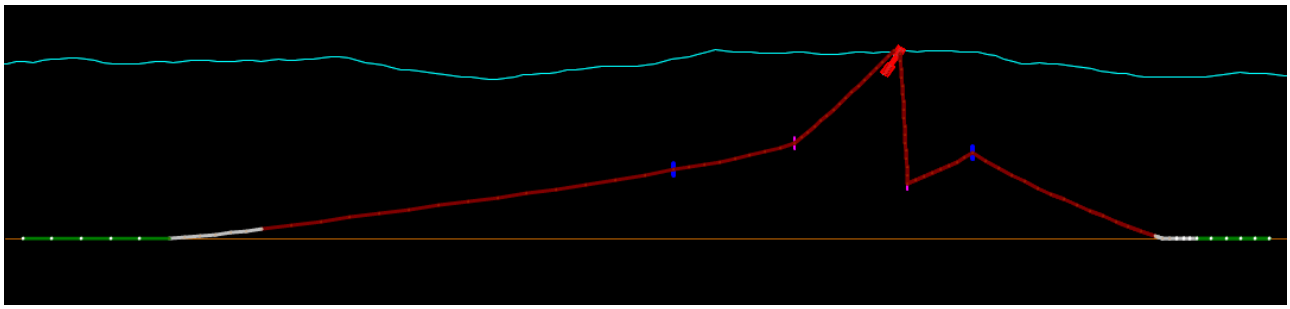

FIGURE 5-2 ORCAFLEX SCREENSHOT: OWC 1 BEHAVIOUR IN 100-YR STORM

A set of data was extracted from each simulation. In particular, the time series of the effective tension at each fairlead as well as the 3D components of the total mooring force in the local coordinate system were obtained. The local coordinate system is the coordinate system which coincides with the global coordinate system when the buoy is at equilibrium position, but it translates and rotates with the buoy.

Two results were issued from those data; on the one hand, the maximum (over the 10 sets of 3-hour simulations) of the local 3D components of the total mooring force is provided for input of the 1D beam model of the OWC. On the other hand, the maximum (over the 10 sets of 3-hour simulations) of the effective tension at the fairlead is provided for detailed design of the structure. The results of this study are provided in Table 5-5.

TABLE 5-5 MOORING LOADS IN 100-YR STORM

Maximum Effort	3 m diameter	6 m diameter	12 m diameter
Lx (N)	4.322E+05	2.097E+06	4.896E+06
Ly (N)	7.567E+03	3.060E+03	4.239E+05
Lz (N)	5.707E+05	1.816E+06	5.675E+06
Effective tension (N)	6.257E+05	2.063E+06	4.800E+06

NB: A safety factor of 1.3 is to be applied to those values.

5.3. Methodology for the structural analysis

This section presents the methodology for the preliminary structural assessment. The final objective of this methodology is to provide a framework for the comparison of the 3 versions of the proposed system. At a later stage of the system development, a more complete

methodology should be elaborated for the assessment of general dynamics, external loads, internal loads and structural assessment.

Figure 5-3 presents the preliminary verification process detailed in the following sections.

If design is modified, external loads (except structural weight) and motion related quantities (e.g. max pitch angle) will not be updated by INNOSEA as they are provided by IST and WAVEC (section 5.3.3). A loop might be needed after refinement of the scantling.

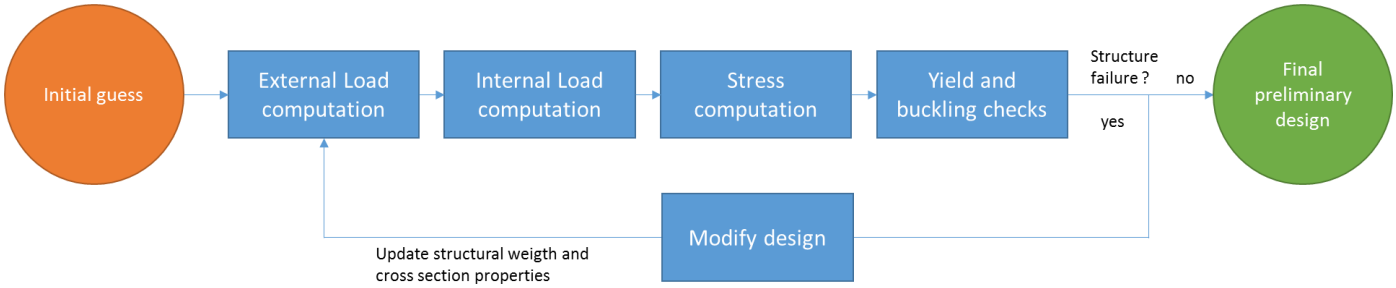

FIGURE 5-3 PROCESS TO PROVIDE THE FINAL PRELIMINARY DESIGN FROM INITIAL GUESS

5.3.1. Choice of methodology for preliminary structural assessment of the OWC spar buoy

The preliminary structural analysis proposed here will be based on simplified method for the following reasons:

- The design is a conceptual stage, therefore there is much uncertainties in the data at this stage.
- Different design configurations need to be assessed quickly.
- The scantling of the design is not known and the purpose of this analysis is to get a first estimation of it. Iteration loops on the scantling will be performed and need to be quick.

In the following subsections the proposed methodology for this preliminary structural assessment of the OWC spar buoy is highlighted.

For this preliminary structural assessment, the OWC spar buoy is modelled as a beam. It is assumed that the structure is slender enough to be considered as a beam for the evaluation of internal structural loads. On this specific topic, at a later stage of system development, structural verification should be performed with FEM model and shell elements. These loads are then derived into stresses to perform the structural assessment. Regarding the structural analysis, general and local verifications are included. Beam and shell failure modes are considered. Analytical calculations are performed based on reference standards (section 5.3.1).

In this preliminary study, only Ultimate Limit State (ULS) will be considered for a limited number of load cases considered potentially critical at this stage. Fatigue will not be considered at this stage. On this specific topic, at a later stage of system development, Fatigue Limit State (FLS) verification should be performed

The spar structure is divided into slices as presented by Figure 5-4.

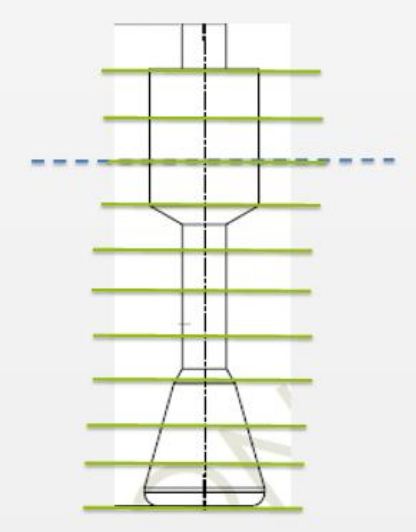

FIGURE 5-4 SLICES ALONG THE HULL

Each slice is assumed to have constant properties (diameter, thickness, material).

5.3.2. Code and standards

The proposed methodology for the preliminary structural assessment of the OWC Spar Buoy refers to a number of standards:

- DNV-OS-C106 "Structural Design of Deep Draught Floating Units (LRFD Method)" [41] gives guidelines on deep draught floating units structural design.
- DNV-RP-F205 "Global Performance Analysis of Deepwater Floating Structures" [42] presents the guidelines on floating structure design regarding motions and external loads.
- DNV-OS-C101 "Design of Offshore Steel Structures, General (LRFD Method)" [43] presents a list of structural checks for steel to be studied.
- DNV-RP-C202 "Buckling Strength of Shells" [44] presents a methodology to assess the buckling limit stress of cylinder shells.

These guidelines are used only for some aspects, at this preliminary verification stage, the methodology is not compliant with these guidelines.

5.3.3. External load modelling

The only external load calculated by INNOSEA is the structural weight.

All the other external loads (except structural weight) will be provided by IST and WAVEC.

Inertial loads should normally be considered for the structural analysis, especially under large pitch angle as provided by IST. However if structure motion and accelerations are not provided to INNOSEA, static equilibrium will be assumed and dynamic inertial loads will be neglected. This is a substantial assumption for the design of floating structure. On this specific topic, at a later stage of system development, more investigation will be needed.

All external loads will be assessed by slice along the height of the OWC spar buoy.

Corrosion and marine growth are not considered for this preliminary verification (this should be considered in a later stage).

5.3.4. Internal load assessment

Beam theory is applied for the calculation of internal loads.

The main assumptions of beam theory are:

- The beam is initially straight, of constant section and such as the length of the beam is large compared to its diameter.
- Material of beam is homogenous and isotropic.
- Young's modulus is constant in compression and tension.
- Transverse section which are plane before bending remain plain after bending.
- Radius of curvature is large compared with dimension of cross sections.
- Each layer of the beam is free to expand or contract.

A static equilibrium of the structure is assumed. Both structure ends are assumed to be free.

Equilibrium of each slice submitted to external and internal loads is solved. Doing so, the internal load in each slice is obtained. All the calculations are analytical.

5.3.5. Stress assessment

From internal loads, the stress assessment is performed following the methodology of DNV-OS-C106 [41] which refers to DNV-OS-C101 [43].

For the LTT, structural properties of concrete inside ballast zone are neglected. This assumption may have to be revised depending on the results.

5.3.6. Limit stress

Yielding is checked by comparing Von Mises stress σ_{VM} to the yield limit stress of the material σ_y.

Buckling is checked by comparing Von Mises stress σ_{VM} to the buckling limit stress, which is itself computed in accordance to DNV-RP-C202 [44] (as referred by DNV-OS-C101 [43]).

6. POTENTIAL CHALLENGES

6.1.Structural engineering challenges

The OWC Spar-Buoy is a long floating structure made of thin cylindrical panels. Some expected critical structural aspects (non-exhaustive) are listed below:

As mentioned by DNV-OS-C106 [41], large bending moment might occur in a Spar, in particular in case of pitch angle. Bending moment may be critical for the small thickness tube. Some load cases may lead to important bending moment [41], among them dry lifting, transportation and operation with large pitch angle.

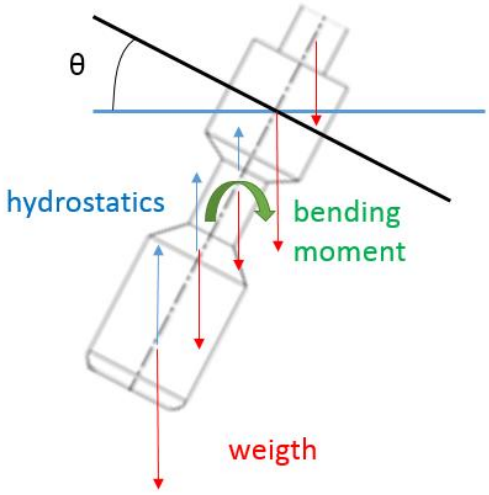

FIGURE 6-1 P-Δ EFFECT DUE TO PITCH ANGLE

High pressure differences due to the hydrostatic pressure might be important for the floater and the large thickness tube. For this reason, presence of air in the large thickness tube could lead high loads.

Buckling may be more critical than yield for thin panels. The ultimate strength may be significantly reduced because of buckling.

If substantial thickness increases are required, the following points may be critical:

- Increase of thickness may lead to excessive structure mass that could impact system performance.
- Excessive thicknesses may lead to unfeasible designs from a manufacturing point of view.

For these reasons, it could be interesting to change the structure arrangement by adding longitudinal and/or ring stiffeners. Doing so, it might lead to smaller mass increase. However, in case such stiffeners were in contact with water, it might alter the hydrodynamic behavior of the system.

6.2. Environmental impacts

This section of the report aims to define a methodology to quantify the potential environmental impacts of the described breakthroughs, focusing on their features and on the general characteristics of the sites where they are supposed to be installed. The environmental impact analysis will be based on literature available and on experience of impacts assessment get so far for WEC projects in order to identify the key inputs and indicators to be assessed in WP7 of the WETFEET project.

The Environment Impact Assessment is a well-known tool, widely accepted to understand and quantify the impacts of human activities. Its application is nowadays incorporated in numerous national regulations for licensing human activities, including wave energy harnessing. The main steps of the EIA approach are presented in Figure 6-2. It is not possible to apply the full EIA methodology herein (e.g. screening, public involvement), since no sufficient socio-environmental data is available for the Leixões site under analysis in chapters 5 & 6. However, the methodology will consider the techniques involved to address some of them namely scoping, impact analysis, mitigation measures, and monitoring activities.

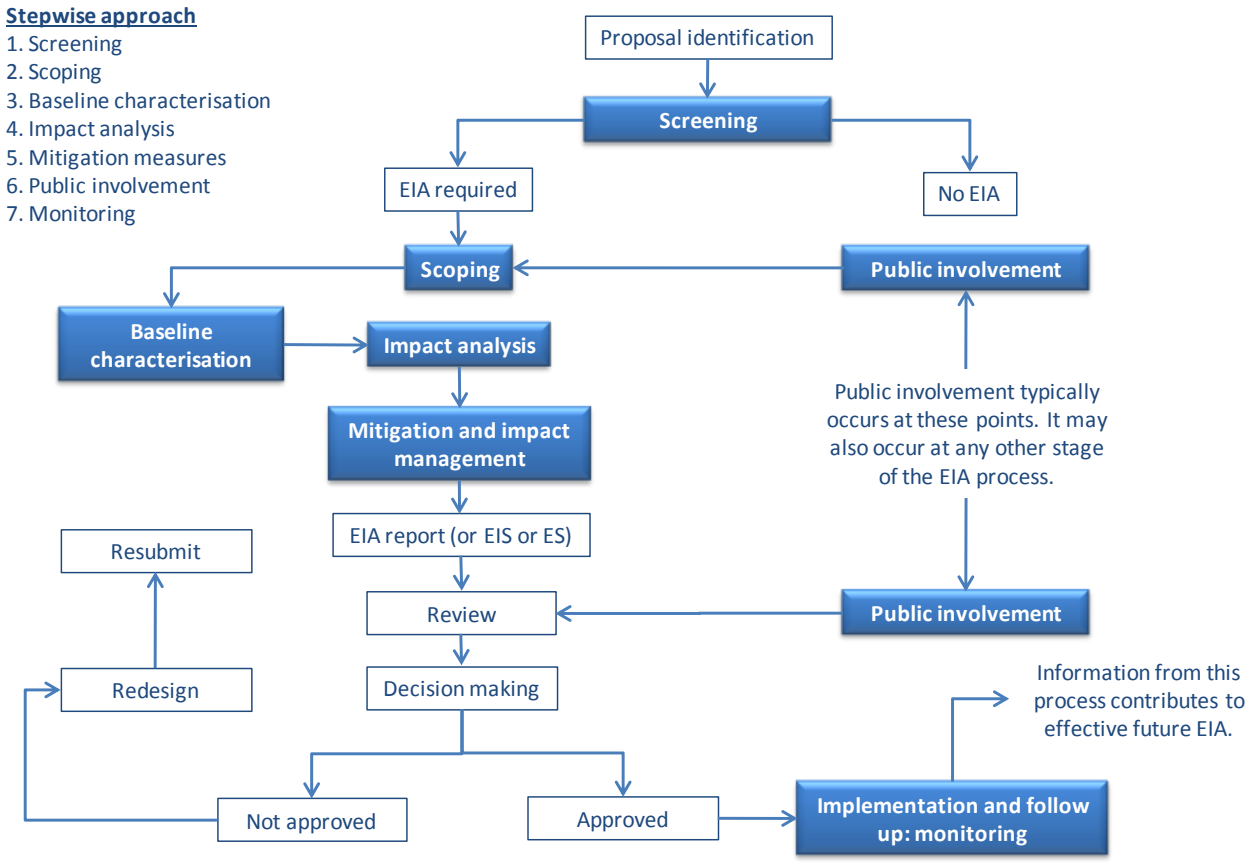

FIGURE 6-2 THE ENVIRONMENTAL IMPACT ASSESSMENT STEPWISE APPROACH: THEORETICAL STEPS

The Scoping process is an essential step of the EIA, which aims to identify, at an early stage of the project development, the key environmental issues that will need most attention. Environmental key issues are e.g. environmental receptors significantly affected, effects or potential impacts of the project on the environment, environmental issues that need detailed study (both desk study and or baseline survey), methodologies to use, possible mitigation measures, constraints that may pose problems and whom to consult with. During this process, a number of potential environmental and socio-economic potential impacts can be avoided through amendments to the e.g. choice of location, technology and materials [45]. One of the approaches that has been proposed is the preliminary identification of stressors (features of the environment that may change with project implementation) and receptors (ecosystem elements with potential for some form of response to the stressor) [46], [47]. Table 6-1 shows a preliminary analysis of the key stressors and receptors to be considered in the breakthroughs which will then be taken into account during the scoping exercise.

TABLE 6-1 PRELIMINARY IDENTIFICATION OF KEY STRESSORS AND ENVIRONMENTAL RECEPTORS OF THE BREAKTHROUGHS CONSIDERED.

Breakthroughs		Key stressors	Key receptors
Improved power conversion	Dielectric Elastomer Generators (DEG)	Collision (elastic stretch) Alteration of water quality (corrosion of new materials)	Marine mammals Fish Benthos
	Tetra-radial turbine	Noise Collision	Marine mammals Fish
Optimized structural design and device profile	Negative Spring (NS) Enhanced Added-Mass (EAM) Survivability submergence	Artificial reef effect Collision Entanglement Hydrodynamic alterations	Sediment dynamics (seabed morphology) Marine mammals Fish Benthos
Array optimization	Shared moorings with rigid connections Shared moorings with non-rigid connections	Collision Entanglement Artificial reef effect	Marine mammals Fish Benthos
Increased system reliability	Submergence under harsh environmental conditions DEG endeavour	Collision Entanglement Noise	Marine mammals Fish

The effects of such stressors on the receptors will then be identified (impacts identification; both negative and positive) and quantified (impacts analysis) based on experience related with similar projects or simply based on expert knowledge regarding the sensitivity of the site and project characteristics. The impacts quantification will, as far as possible, be based on the criteria presented in Table 6-2.

TABLE 6-2 EXAMPLES OF CRITERIA TO BE USED IN THE ENVIRONMENTAL IMPACTS EVALUATION OF THE BREAKTHROUGHS.

Criteria	Qualitative grade
Nature of impact	Direct, indirect
Signal	Positive, neutral, negative
Magnitude (severity)	Maximal, moderate, minimal
Probability of occurrence	High, medium, low
Duration	Temporal, intermittent, permanent
Frequency / Periodicity	Continuous, discontinuous, periodic (e.g. seasonal), regular occurrence, rare
Temporal extension	Immediate, short-term, medium -term, long-term
Spatial extension	Local, adjacent, regional, national, global
Recoverability	Irrecoverable, irreversible, reversible, recoverable, fugal
Inter-relations between actions and effects	Simple, cumulative, synergetic
Need for mitigation measures	Critical, severe, moderate, partial, no-mitigation
Importance (significance)	High significance, significant, low significance, irrelevant

Most of the times information for impacts quantification is not available. Thus the environmental impacts assessment of the breakthroughs will be based on a risk analysis relying on the risk probability of a given impact to occur. A final table of the key impacts identified together with mitigation measures and monitoring activities will finally be presented for each of the breakthroughs considered. The application of this EIA methodology will be carried out within the work package 7 of the WETFEET project.

6.3.Cost implications

The breakthroughs here proposed are to be developed and studied within WETFEET, in order to assess if these act as expected in terms of improved performance, reliability and survivability, in a way that is not detrimental to the overall cost of energy.

It is expected that these breakthroughs will bring improvements in different criteria, which may have implications in terms of the overall cost of the system.

In order to assess the feasibility of these breakthroughs, their costs must be weighed against the benefits they bring. The benefits from each breakthrough may range from added electricity output, higher power quality, higher survivability and reliability to geospatial optimization. The benefit of a breakthrough may also be directly applied on the costs, as lower initial cost or less costly maintenance.

Cost-benefit analysis is a common technique to estimate the strengths and weaknesses of different alternatives, allowing for an easier comparison and to aid in the process of decision-making. Regarding energy technologies, it is common to weigh the costs against the energy production[2]. The chosen indicator by renewable energy developers to assess the feasibility of their solutions is the Levelized Cost of Electricity, as it allows not only the comparison between alike technologies, but also with those that use other sources, including fossil fuels.

As indicated by the International Energy Agency (IEA), *the notion of levelized costs of electricity (LCOE) is a handy tool for comparing the unit costs of different technologies over their economic life. It would correspond to the cost of an investor assuming the certainty of production costs and the stability of electricity prices* [48].

Furthermore it is an indicator that is understandable by both developers and investors, as it is comparable to the market electricity selling price, but requires fewer inputs than financial indicators such as Net Present Value (NPV) and the Internal Rate of Return (IRR).

Concretely, LCOE is defined as the total lifecycle costs (i.e., the sum of all capital costs and lifetime operation and maintenance costs, discounted to present value) divided by the electricity generation to grid accumulated throughout the technology's lifetime (also discounted to present value)[49]. A common representation of this is shown in (6.1).

$$LCOE = \frac{\sum_{t=0}^{n} \frac{(Investment_t + O\&M_t + Fuel_t + Carbon_t + Decommissioning_t)}{(1+r)^t}}{\sum_{t=0}^{n} \frac{AEP_t}{(1+r)^t}} \quad (6.1)$$

$LCOE$ = *Levelized Cost of Electricity*
AEP_t = Annual electricity production *(at year t)*
r = Discount rate

[2] Which is the direct benefit for the user of the technology.

n = Lifetime of the system
t = Project year, from the start of the project (*year 0*) to the final year of the project (*year n*)

This equation can be used for different energy systems, and other cost centres can be added as needed. For renewable energy systems, which have no fuel or carbon costs, it is common to simplify the equation down to:

- Investment costs, commonly called **CAPEX**: these are assumed to happen all in year 0, for the simplicity of the calculation. However this value can be adjusted to account the time it takes to develop a project. Investment costs can also be divided into procurement costs (cost of purchasing the elements in a project), installation costs and administrative costs.
- Operational costs, commonly called **OPEX**: all the cost incurred during the operational lifetime of the project. For more simple calculations these are can be assumed as fixed rate throughout the lifetime of the project. However, operational costs are not fixed. There will be a part of fixed costs related to administrative and other recurrent costs, but maintenance operations, especially corrective ones, will had a variable element to the operational costs.
- Decommissioning costs are sometimes included in the OPEX, but it is common that decommissioning costs are not included, as due to the nature of the present value calculation, its impact on the LCOE is very small.

On the denominator side, the Annual Energy Production (**AEP**) has the role of offsetting the costs.

Finally, the discount rate is a measure of time-value, which is the price put on the time that an investor waits for a return on an investment. Furthermore, the discount rate is also used to account for the risks and uncertainties of an investment. For a specific project, the discount rate will be a product of the project developer's (or investors) desired return on investment[3] and the inherent risks of the project that will not only be related to the technology being deployed but also to the market it will be deployed in [49]–[51].

With the knowledge of how the LCOE is calculated, the breakthroughs proposed in WETFEET can be assessed by their impact on the different inputs of the equation. Higher added CAPEX may be offset by higher electricity production or by higher reliability, which translates in lower OPEX costs. Furthermore, the survivability of the device has an influence on the perceived risk of the technology, which also has an impact on the LCOE, via a lower discount rate.

[3] This is associated with the weighted average cost of capital (WACC), which determines how much the developer has to pay for others to supply the funds to advance the project. This can come from debt (the cost of capital is the interest rate), equity (with varying costs of capital depending on company profile) and from public funding (which may have a 0 cost of capital).

Current wave technologies are often assessed using a 10-15% discount rate, aiming that first and second arrays may be in the range of 8-10%. The impact of the discount rate, using 15% as reference, is presented on Figure 6-3.

FIGURE 6-3 IMPACT OF THE DISCOUNT RATE ON THE LCOE

In work package 7 the full impacts will be studied and the contribution to the LCOE will be assessed.

However, it is possible to broadly estimate the expected contribution of each breakthrough in the different LCOE components. Table 6-3 presents the expected contributions on the different components of the LCOE. Confirmation of these expectations will be determined as part of the techno-economic analysis to be carried out in work package 7.

TABLE 6-3 EXPECTED IMPACTS OF THE DIFFERENT BREAKTHROUGHS ON THE LCOE COMPONENTS

Breakthrough concept	Expected impact on the AEP	Expected impact on the CAPEX	Expected impact on the OPEX
Dielectric Elastomer Generators (DEG)	⇧	⇩	⇩
Tetra-radial turbine	⇧	0	0
Negative Spring (NS)	⇧	0	0
Enhanced Added-Mass (EAM)	⇧	⇧	0
Survivability submergence	⇧	⇧	⇩
Shared moorings	0	⇩	⇩

7. CONCLUSIONS AND FUTURE WORK

In this deliverable, preliminary design and breakthroughs integration considerations were depicted with respect to the development of an OWC spar buoy WEC. The potential challenges raised in the previous chapter will serve as a basis on the decision to select the most appropriate configurations of the OWC spar buoy for each breakthrough.

Following this work, an iterative process between the structural loads calculation (initiated in section 5.2) and the structural analysis method developed in section 5.3 will occur in order to gather sufficient information on the structural challenges associated with the three geometries of the reference case OWC spar buoy (without featuring any breakthroughs). On the one hand, this will facilitate bringing down the number of design configurations to be investigated per OWC spar buoy featuring one of the breakthrough concepts. On the other hand, this will provide a relevant set of data to discuss on the feasibility and performance of the proposed breakthrough against the reference case.

Beyond the conceptual and preliminary analysis reported in the present document, the following future steps will be undertaken to further develop the breakthrough ideas related to the OWC spar buoy:

- Negative springs: the impact on motion and performance introduced by both the IVV and HNS methods will be investigated. To this extent, linear wave theory will first be explored for one geometry of the OWC spar buoy. Due to the non-linear effects associated with the HNS method, a partial time-domain code will also be utilized. Finally, the most promising configurations may be the object of CFD simulations if time allows. This work will be carried out jointly under work packages 2 & 3 (with reference to the tasks 2.2, 2.3, 2.4 & 3.2).
- Enhanced added-mass: alternative optimization schemes than the one proposed in Gomes et al. [12] will be established to reflect stability criteria and/or cost implications. Both the design variable and associated constraints as well as the objective function will be modify to further analyse the submerged mass located at the bottom of the OWC spar buoy.
- Submergence for survivability: various submergence depth levels will be analysed by both the linear frequency-domain WAMIT code and the non-linear Ship@Sea code for one geometry of the OWC spar buoy (i.e one of the three diameters explored in this report). Dynamic behaviour and mooring forces under full submergence of the OWC

spar buoy will be further studied using the commercial Orcaflex™. A connection with task 3.1 will be made to ensure continuity of the workflow about this breakthrough

- Dielectric elastomer generators: it is intended to engage the coupling effort between the hydrodynamic and electro-mechanical modelling of the proposed architectures for the OWC spar buoy featuring DEG. The two OWC spar buoy DEG configurations proposed in Figure 3-4 will be studied assuming one fixed diameter for comparison purposes. A Finite Element Method tool will be used to have a more accurate estimation of the DEG membrane dimensions for the two OWC spar buoy configurations.

The other two breakthrough concepts (tetra-radial air turbine and array breakthroughs) considered in this report will not be the object of further work within the frame of the work package 2 since they have dedicated tasks already engaged respectively in work packages 4 & 6.

The overriding goal of the work which is developed in the present deliverable and the subsequent deliverable 2.3 is to shoulder the technical judgement of the breakthroughs ideas into the OWC spar buoys. For this purpose, specialized numerical tools are exploited allowing statements with respect to the technical performance and design suitability of the proposed configurations. Ultimately, this work serves as a basis to carry on the assessment of the most auspicious breakthrough ideas in the remaining of the WETFEET project.

BIBLIOGRAPHY

[1] N. Delmonte, D. Barater, F. Giuliani, P. Cova, and G. Buticchi, "Review of Oscillating Water Column Converters," *IEEE Trans. Ind. Appl.*, 2015.

[2] F.-X. Faÿ, J. C. C. Henriques, M. Marcos, and E. Robles, "Review of control strategies for oscillating water column wave energy converters," in *11th European Wave and Tidal Energy Conference*, 2015, no. 1.

[3] T. V. Heath, "A review of oscillating water columns," *Philos. Trans. R. Soc. A Math. Phys. Eng. Sci.*, vol. 370, no. 1959, pp. 235–245, 2012.

[4] A. F. de O. Falcão and P. A. . Justino, "OWC Wave energy devices with air-flow control," *Ocean Eng.*, vol. 26, pp. 1275–1295, 1999.

[5] A. F. de O. Falcão and J. C. C. Henriques, "Oscillating-water-column wave energy converters and air turbines: A review," *Renew. Energy*, vol. 85, pp. 1391–1424, 2016.

[6] S. . Crowley, R. Porter, and D. . Evans, "A submerged cylinder wave energy converter with internal sloshing power take off," *Eur. J. Mech. - B/Fluids*, vol. 47, pp. 108–123, 2014.

[7] A. Kurniawan, D. Greaves, and J. Chaplin, "Wave energy devices with compressible volumes," *Proc. R. Soc. A*, vol. 470, 2015.

[8] M. E. McCormick, "Analysis of wave energy conversion buoy," *J. Hydronautics*, vol. 8, no. 3, pp. 77–82, 1974.

[9] M. E. McCormick, "A modified linear analysis of wave energy conversion buoy," *Ocean Eng.*, vol. 3, no. 3, pp. 133–144, 1976.

[10] T. W. T. Whittaker and F. A. Mc Peake, "Design Optimization of Axi-symmetric Tail Tube Buoys," in *International Union of Theoretical and Applied Mechanics*, D. . Evans and A. F. de O. Falcão, Eds. Berlin, Germany: Springer, 1986.

[11] DTI, "Near Shore Floating Oscillating Wave Column: Prototype Development and Evaluation," 2004.

[12] R. P. F. Gomes, J. C. C. Henriques, L. M. C. Gato, and A. F. de O. Falcão, "Hydrodynamic optimization of an axisymmetric floating oscillating water column for wave energy conversion," *Renew. Energy*, vol. 44, pp. 328–339, 2012.

[13] A. F. de O. Falcão, J. C. C. Henriques, and J. J. Cândido, "Dynamics and optimization of the OWC spar buoy wave energy converter," *Renew. Energy*, vol. 48, pp. 369–381, 2012.

[14] A. F. de O. Falcão, J. C. C. Henriques, L. M. C. Gato, and R. P. F. Gomes, "Air turbine choice and optimization for floating oscillating-water-column wave energy converter," *Ocean Eng.*, vol. 75, pp. 148–156, 2014.

[15] D. Bull and M. E. Ochs, "Technological Cost-Reduction Pathways for Oscillating Water Column Wave Energy Converters in the Marine Hydrokinetic Environment," 2013.

[16] J. V Ringwood and G. Bacelli, "Energy-Maximizing Control of Wave-Energy Converters," *IEEE Control Syst. Mag.*, vol. 35, no. October, pp. 30–55, 2014.

[17] F. Paparella, K. Monk, V. Winands, M. Lopes, D. Conley, and J. V. Ringwood, "Up-wave and autoregressive methods for short-term wave forecasting for an oscillating water column," *IEEE Trans. Sustain. Energy*, vol. 6, pp. 171–178, 2015.

[18] J. C. C. Henriques, R. P. F. Gomes, L. M. C. Gato, A. F. de O. Falcão, E. Robles, and S. Ceballos, "Testing and control of a power take-off system for an OWC spar-buoy wave energy converter," *Rewable energy*, vol. 85, pp. 714–724, 2014.

[19] F. X. C. Fonseca, "Testing of a 1:32 scale model of a floating oscillating water column system for wave energy conversion," Instituto Superior Técnico, University of Lisbon, 2014.

[20] K. Budal and J. Falnes, "A resonant point absorber of ocean-wave power," *Nature*, vol. 256, pp. 478–479, 1975.

[21] D. V Evans, "A theory for wave-power absorption by oscillating bodies," *J. Fluid Mech.*, vol. 77, no. 1, pp. 1–25, 1976.

[22] J. Falnes, *Ocean Waves and Oscillating Systems*. Cambridge University Press, 2002.

[23] J. Hals Todalshaug, "Wave Energy Convertor," WO 2015107158 A12015.

[24] "CorPower Ocean," 2015. [Online]. Available: http://www.corpowerocean.com. [Accessed: 01-Dec-2015].

[25] J. Hals Todalshaug, G. Steinn Àsgeirsson, E. Hjálmarsson, P. Pires, M. Guérinel, J. Maillet, M. Lopes, and P. Möller, "Tank testing of an inherently phase controlled Wave Energy Converter .," in *11th European Wave and Tidal Energy Conference*, 2015.

[26] S. Peretta, P. Ruol, L. Martinelli, A. Tetu, and J. P. Kofoed, "Effect of a negative stiffness mechanism on the performance of the WEPTOS rotors," in *6th International Conference on Computational Methods in Marine Engineering*, 2015.

[27] X. Zhang and J. Yang, "Power capture performance of an oscillating-body WEC with nonlinear snap through PTO systems in irregular waves," *Appl. Ocean Res.*, vol. 52, no. AUGUST, pp. 261–273, 2015.

[28] X. Zhang, J. Yang, and L. Xiao, "Numerical Study of an Oscillating Wave Energy Converter with Nonlinear Snap - Through Power - Take - Off Systems in Regular Waves," in *33rd International Conference on Ocean Offshore Arctic Engineering*, 2014, pp. 225–230.

[29] M. Guerinel, A. S. Zurkinden, M. Alves, and J. N. A. Sarmento, "Validation of a partially nonlinear time domain model using instantaneous Froude-Krylov and hydrostatic forces," in *European Wave and Tidal Energy Conference, EWTEC*, 2013.

[30] M. Peñalba Retes, A. Merigaud, J. Gilloteaux, and J. V. Ringwood, "Nonlinear Froude-Krylov force modelling for two heaving wave energy point absorbers," in *10th European Wave and Tidal Energy Conference*, 2015, pp. 1–10.

[31] M. Peñalba Retes, G. Giorgi, and J. V Ringwood, "A Review of non-linear approaches for wave energy converter modelling," in *11th European Wave and Tidal Energy Conference*, 2015, no. 1, pp. 1–10.

[32] S. Ribeiro E Silva and C. Guedes Soares, "Prediction of parametric rolling in waves with a time domain non-linear strip theory model," *Ocean Eng.*, vol. 72, pp. 453–469, 2013.

[33] L. M. C. Gato, A. F. de O. Falcão, J. C. C. Henriques, R. P. F. Gomes, P. Vicente, F. Fonseca, J. Varandas, and L. Trigo, "MARINET Report - Dynamics of oscillating water column spar-buoy wave energy converters deployed in array and its survivability in extreme conditions," 2015.

[34] J. C. C. Henriques, A. F. de O. Falcão, R. P. F. Gomes, and L. M. C. Gato, "Latching control of an OWC spar-buoy wave energy converter in regular waves," *J. Offshore Mech. Arct. Eng.*, vol. 135, pp. 56–64, 2013.

[35] J. C. C. Henriques, L. M. C. Gato, A. F. de O. Falcão, E. Robles, and F.-X. Faÿ, "Latching control of a floating oscillating-water-column wave energy converter," *Renew. Energy*, vol. 90, no. JANUARY, pp. 229–241, 2016.

[36] A. F. de O. Falcão, L. M. C. Gato, and E. P. a S. Nunes, "A novel radial self-rectifying air turbine for use in wave energy converters. Part 2. Results from model testing," *Renew. Energy*, vol. 53, pp. 159–164, 2013.

[37] A. F. de O. Falcão, L. M. C. Gato, J. C. C. Henriques, J. E. Borges, B. Pereiras, and F. Castro, "A novel twin-rotor radial-inflow air turbine for oscillating-water-column wave energy converters," *Energy*, vol. 93, pp. 2116–2125, 2015.

[38] Statoil, "Statoil - HyWind demo," 2009. [Online]. Available: http://www.statoil.com/no/TechnologyInnovation/NewEnergy/RenewablePowerProduction/Offshore/Hywind/Pages/HywindPuttingWindPowerToTheTest.aspx.

[39] Statoil, "Statoil - Innovate challenge on the installation methods for the HyWind," 2012. [Online]. Available: http://innovate.statoil.com/challenges/hywind/pages/default.aspx.

[40] Det Norske Veritas, "DNV-RP-C205 Environmental Conditions and Environmental Load," 2010.

[41] *DNV-OS-C106: Structural Design of Deep Draught Floating Units / Spars*, vol. DNV-OS-C10. 2012.

[42] *DNV-RP-F205: Global Performance Analysis of Deepwater Floating Structures*, vol. DNV-RP-F20. 2009.

[43] Det Norske Veritas, "DNV-OS-C101 Design of Offshore Steel Structures - General (LRFD Method)," 2011.

[44] *DNV-RP-C202: Buckling Strength of Shells*, vol. DNV-RP-C20. 2013.

[45] T. C. Simas, A. C. Moura, D. Thompson, R. S. Batty, J. Norris, and G. Harrison, "Environmental Assessment for Ocean Energy Schemes: Useful Tools and Case Studies," in *The Proceedings of the 20th (2010) International Offshore and Polar Engineering Conference*, 2010.

[46] G. McMurray, "Wave energy ecological effects workshop ecological assessment briefing paper," *Ecol. Eff. Wave Energy Dev. Pacific Northwest*, p. 25, 2008.

[47] G. W. Boehlert and A. B. Gill, “Environmental and ecological effects of ocean renewable energy development: a current synthesis,” 2010.

[48] IEA, “Projected Costs of Generating Electricity,” 2010.

[49] W. Short and D. J. Packey, “A Manual for the Economic Evaluation of Energy Efficiency and Renewable Energy Technologies,” 1995.

[50] Carbon Trust, “Cost estimation methodology,” 2006.

[51] “Discount rates for low carbon and renewable generation technologies,” Committee on Climate Change, Apr. 2011.

APPENDICES

A. Hydrostatic and dynamic wave loads – theory

Let the complex fluid velocity potential be:

$$\varphi = \underline{\varphi} e^{i\omega t}$$

With $\underline{\varphi} = We^{\delta}$ where W is the modulus and δ the phase. The same notation is used for all the other complex quantities defined in this document.

WAMIT provides the user with the complex value of the hydrodynamic pressure on each panel according to the following formula:

$$p = -\frac{\partial \varphi}{\partial t}$$

Where p is the hydrodynamic pressure and φ is the fluid potential. Because the body is at rest, in this case the total fluid potential is equal to the diffraction potential defined by:

$$\varphi = \varphi_I + \varphi_7$$

Where φ_I is the fluid potential associated to the incoming wave and φ_7 is the potential of the fluid scattered by the body.

It is important to note that the central column of the OWC spar buoy was defined by so-called "dipole panels", on which is calculated the pressure jump between the two sides of the panel.

Therefore, the efforts consider the contribution of the hydrodynamic pressure both on the outer and inner surface of the water column, and the components of the efforts on a slice are given by:

$$Re(F_x) = \iint_{S_{IN}\ U\ S_{OUT}} Re(p)\,.\,n_x\,dS$$

$$Im(F_x) = \iint_{S_{IN}\ U\ S_{OUT}} Im(p)\,.\,n_x\,dS$$

Where S_{IN} is the surface of the inner boundary of the OWC spar buoy for the considered slice and S_{OUT} is the surface of the outer boundary of the OWC spar buoy. Normals are pointing towards the body. The same goes for F_y and F_z. Classic relations between modulus, phase, real and imaginary parts of theses component apply. In particular:

$$|F_x| = sqrt(\ Re(F_x)^2 + Im(F_x)^2\ )$$

And

$$\arg\,(F_x) = \arctan\,(\ Im(F_x)\ \ /Re(F_x)\ \ )$$

In the case of a dipole panel, WAMIT® provides the user with the pressure jump between outer and inner boundaries. Consequently, the contributions at the central column are computed through the following:

$$Re(F_x) = \iint_S Re(\Delta p)\,.\,n_x\,dS$$

$$Im(F_x) = \iint_S Im(\Delta p)\,.\,n_x\,dS$$

Where S is the surface of the outer boundary of the column for the considered slice.

The hydrostatic contribution is also provided. It is pointing vertically and was calculated per slices through the following formula:

$$Re(F_{HS}) = \iint_{S_{IN}\ U\ S_{OUT}} -\rho g z\,.\,n_z\,dS$$

B. Orcaflex settings

TABLE B-1 ORCAFLEX SETTINGS

Setting	Value	Unit	Comment
Integration scheme	Implicit	-	Variable time step
Time step	0.25	s	Maximum value
Simulation length	10800	s	
Vessel Hydrodynamics	Morison	-	
Wave and current direction	0	deg	Collinear, aligned with ML1
Targeted mooring line segment	[3-5-10-5-10]	m	per section (from vessel to anchor)

C. Hydrostatic and dynamic wave loads – Results

TABLE C-1 RAW RESULTS - WAVE LOADS IN 100-YR STORM – 3 M DIAMETER OWC SPAR BUOY

Z Slice center	Fx (hydrodynamic pressure)		Fy (hydrodynamic pressure)		Fz (hydrodynamic pressure)		Fz_hs (static pressure)
(m)	Mod (N)	Phase (rad)	Mod (N)	Phase (rad)	Mod (N)	Phase (rad)	(N)
-8.894	2.772E+03	1.571	8.377E-02	0.006	6.402E+05	0.001	4.692E+05
-8.704	3.539E+03	1.571	3.860E-01	0.003	9.533E+04	0.001	6.794E+04
-8.503	5.527E+03	1.571	3.116E-01	3.139	4.072E+03	0.001	2.855E+03
-8.289	4.745E+03	1.571	3.507E-01	3.139	0.000E+00	0.000	0.000E+00
-8.096	4.915E+03	1.571	6.034E-01	-3.132	0.000E+00	0.000	0.000E+00
-7.887	6.751E+03	1.571	2.446E-01	0.019	0.000E+00	0.000	0.000E+00
-7.679	5.162E+03	1.571	3.707E-01	0.025	0.000E+00	0.000	0.000E+00
-7.487	5.234E+03	1.571	6.721E-01	-3.133	0.000E+00	0.000	0.000E+00
-7.294	5.292E+03	1.571	3.867E-01	-3.133	0.000E+00	0.000	0.000E+00
-7.085	7.128E+03	1.571	1.254E+00	0.019	0.000E+00	0.000	0.000E+00
-6.876	5.386E+03	1.571	1.942E+00	-3.131	0.000E+00	0.000	0.000E+00
-6.685	5.412E+03	1.571	1.001E+00	0.010	7.015E+01	-3.141	-3.698E+01
-6.492	5.430E+03	1.571	1.608E-01	3.118	1.054E+02	-3.141	-5.419E+01
-6.282	7.255E+03	1.571	2.687E-01	3.101	1.409E+02	-3.141	-6.985E+01
-6.074	5.442E+03	1.571	1.971E-01	-3.137	1.060E+02	-3.141	-5.058E+01
-5.890	5.433E+03	1.571	4.389E-01	0.004	1.063E+02	-3.141	-4.904E+01
-5.698	5.414E+03	1.571	4.361E-01	3.131	1.065E+02	-3.141	-4.749E+01
-5.497	5.381E+03	1.571	5.382E-01	3.129	1.068E+02	-3.141	-4.595E+01
-5.302	7.095E+03	1.571	2.400E+00	0.002	1.428E+02	-3.141	-5.887E+01
-5.103	5.225E+03	1.571	1.719E+00	3.129	1.074E+02	-3.141	-4.235E+01
-4.895	5.595E+03	1.571	1.198E+00	0.011	1.050E+05	-3.141	-3.908E+04
-4.690	4.377E+03	1.571	4.087E-01	0.079	2.226E+05	-3.141	-8.026E+04
-4.492	3.441E+03	1.570	1.330E+00	0.034	1.911E+05	-3.141	-6.583E+04
-4.295	2.616E+03	1.570	1.786E+00	0.038	1.594E+05	-3.141	-5.237E+04
-4.091	2.047E+03	1.569	4.470E+00	0.038	1.112E+05	-3.141	-3.491E+04
-3.903	1.424E+03	1.569	2.180E+00	0.049	0.000E+00	0.000	0.000E+00
-3.716	1.750E+03	1.570	1.426E+00	0.048	0.000E+00	0.000	0.000E+00
-3.509	1.727E+03	1.570	7.828E-01	0.051	0.000E+00	0.000	0.000E+00
-3.302	1.714E+03	1.570	4.350E-01	0.058	0.000E+00	0.000	0.000E+00
-3.095	1.710E+03	1.570	2.080E-01	0.083	0.000E+00	0.000	0.000E+00
-2.888	1.714E+03	1.570	7.897E-02	0.162	0.000E+00	0.000	0.000E+00
-2.702	1.380E+03	1.571	9.746E-03	2.161	0.000E+00	0.000	0.000E+00
-2.516	1.742E+03	1.571	1.325E-01	3.062	0.000E+00	0.000	0.000E+00
-2.309	1.769E+03	1.571	2.729E-01	3.101	0.000E+00	0.000	0.000E+00

Z Slice center	Fx (hydrodynamic pressure)		Fy (hydrodynamic pressure)		Fz (hydrodynamic pressure)		Fz_hs (static pressure)
(m)	Mod (N)	Phase (rad)	Mod (N)	Phase (rad)	Mod (N)	Phase (rad)	(N)
-2.101	1.803E+03	1.571	7.530E-01	3.120	0.000E+00	0.000	0.000E+00
-1.900	2.049E+03	1.571	8.884E-01	3.120	1.909E+05	0.001	2.687E+04
-1.702	3.379E+03	1.571	6.753E-01	3.125	3.382E+05	0.001	4.295E+04
-1.499	5.080E+03	1.571	3.214E-01	3.121	2.081E+05	0.001	2.406E+04
-1.305	5.024E+03	1.571	1.460E-01	3.108	0.000E+00	0.000	0.000E+00
-1.114	5.559E+03	1.571	2.005E-02	3.013	0.000E+00	0.000	0.000E+00
-0.905	6.287E+03	1.571	8.667E-03	2.310	0.000E+00	0.000	0.000E+00
-0.705	5.199E+03	1.571	2.093E-01	3.123	0.000E+00	0.000	0.000E+00
-0.509	6.246E+03	1.571	4.132E-02	0.123	0.000E+00	0.000	0.000E+00
-0.294	6.386E+03	1.571	2.917E-01	3.136	0.000E+00	0.000	0.000E+00
-0.093	5.552E+03	1.571	1.065E-01	0.048	0.000E+00	0.000	0.000E+00

TABLE C-2 RAW RESULTS - WAVE LOADS IN 100-YR STORM - 6 M DIAMETER OWC SPAR BUOY

Z Slice center	Fx (hydrodynamic pressure)		Fy (hydrodynamic pressure)		Fz (hydrodynamic pressure)		Fz_hs (static pressure)
(m)	Mod (N)	Phase (rad)	Mod (N)	Phase (rad)	Mod (N)	Phase (rad)	(N)
-17.886	9.853E+03	1.570	6.387E-01	3.132	2.298E+06	0.002	3.764E+06
-17.703	9.813E+03	1.570	1.544E+00	-0.032	4.821E+05	0.002	7.773E+05
-17.511	2.148E+04	1.570	6.155E-01	3.094	4.909E+05	0.002	7.811E+05
-17.298	1.781E+04	1.570	3.637E+00	3.112	1.507E+05	0.002	2.361E+05
-17.104	2.167E+04	1.570	2.335E+00	-0.030	1.904E+04	0.002	2.950E+04
-16.907	1.923E+04	1.570	9.055E-01	-3.126	1.508E+05	-3.139	-2.262E+05
-16.714	2.440E+04	1.570	5.096E-02	0.262	2.954E+05	-3.139	-4.372E+05
-16.509	2.374E+04	1.570	1.875E-01	0.115	2.870E+05	-3.139	-4.172E+05
-16.309	1.123E+04	1.570	6.155E-01	3.128	1.402E+05	-3.139	-2.012E+05
-16.113	2.252E+04	1.570	1.684E-01	3.078	2.739E+05	-3.139	-3.880E+05
-15.912	2.155E+04	1.570	4.931E-01	0.010	2.651E+05	-3.139	-3.690E+05
-15.704	2.052E+04	1.570	1.421E-01	3.089	2.562E+05	-3.139	-3.504E+05
-15.504	9.685E+03	1.570	3.876E-01	-3.109	6.622E+04	-3.139	-8.493E+04
-15.302	1.895E+04	1.570	2.001E+00	-3.137	1.855E+05	-3.139	-2.429E+05
-15.085	1.787E+04	1.570	2.255E+00	3.128	1.778E+05	-3.139	-2.282E+05
-14.872	1.679E+04	1.570	1.177E+00	0.026	1.700E+05	-3.139	-2.140E+05
-14.696	7.967E+03	1.570	7.788E-01	0.022	7.324E+04	-3.139	-8.987E+04
-14.520	1.518E+04	1.570	5.534E-01	3.132	1.584E+05	-3.139	-1.936E+05
-14.309	1.411E+04	1.571	2.816E+00	-3.121	1.504E+05	-3.139	-1.802E+05
-14.095	1.307E+04	1.570	9.227E-01	-3.126	1.424E+05	-3.139	-1.671E+05
-13.894	6.123E+03	1.570	1.538E+00	0.035	4.441E+04	-3.139	-4.848E+04
-13.691	1.155E+04	1.570	2.797E+00	0.033	1.309E+05	-3.139	-1.493E+05
-13.488	1.010E+04	1.571	3.054E+00	-3.118	1.556E+05	-3.139	-1.773E+05
-13.299	7.897E+03	1.570	5.500E-02	0.334	1.476E+05	-3.139	-1.667E+05
-13.102	8.007E+03	1.570	1.757E-02	1.790	1.541E+05	-3.139	-1.712E+05
-12.900	7.254E+03	1.570	3.473E-01	3.060	1.436E+05	-3.139	-1.567E+05
-12.716	4.022E+03	1.570	1.579E-01	2.934	8.111E+04	-3.139	-8.726E+04
-12.496	9.692E+03	1.570	6.512E-01	3.040	0.000E+00	0.000	0.000E+00
-12.279	4.795E+03	1.570	2.547E-01	3.056	0.000E+00	0.000	0.000E+00
-12.123	4.766E+03	1.570	2.794E-01	3.085	0.000E+00	0.000	0.000E+00
-11.890	9.464E+03	1.570	6.437E-01	3.110	0.000E+00	0.000	0.000E+00
-11.656	4.705E+03	1.570	3.076E-01	3.117	0.000E+00	0.000	0.000E+00
-11.501	4.690E+03	1.570	2.652E-01	3.115	0.000E+00	0.000	0.000E+00
-11.345	4.679E+03	1.570	2.141E-01	3.107	0.000E+00	0.000	0.000E+00
-11.111	9.332E+03	1.570	3.070E-01	3.088	0.000E+00	0.000	0.000E+00
-10.878	4.657E+03	1.570	1.308E-01	3.078	0.000E+00	0.000	0.000E+00
-10.722	4.654E+03	1.570	1.376E-01	3.082	0.000E+00	0.000	0.000E+00

Z Slice center	Fx (hydrodynamic pressure)		Fy (hydrodynamic pressure)		Fz (hydrodynamic pressure)		Fz_hs (static pressure)
(m)	Mod (N)	Phase (rad)	Mod (N)	Phase (rad)	Mod (N)	Phase (rad)	(N)
-10.488	9.304E+03	1.570	3.248E-01	3.095	0.000E+00	0.000	0.000E+00
-10.255	4.653E+03	1.570	1.860E-01	3.104	0.000E+00	0.000	0.000E+00
-10.099	4.656E+03	1.570	1.940E-01	3.106	0.000E+00	0.000	0.000E+00
-9.943	4.660E+03	1.570	1.943E-01	3.107	0.000E+00	0.000	0.000E+00
-9.710	9.336E+03	1.570	3.571E-01	3.105	0.000E+00	0.000	0.000E+00
-9.476	4.678E+03	1.570	1.456E-01	3.098	0.000E+00	0.000	0.000E+00
-9.321	4.687E+03	1.570	1.142E-01	3.089	0.000E+00	0.000	0.000E+00
-9.087	9.403E+03	1.570	1.366E-01	3.061	0.000E+00	0.000	0.000E+00
-8.854	4.718E+03	1.570	3.845E-02	3.001	0.000E+00	0.000	0.000E+00
-8.698	4.731E+03	1.570	3.920E-02	2.996	0.000E+00	0.000	0.000E+00
-8.542	4.745E+03	1.570	5.332E-02	3.023	0.000E+00	0.000	0.000E+00
-8.309	9.535E+03	1.570	1.532E-01	3.047	0.000E+00	0.000	0.000E+00
-8.075	4.793E+03	1.570	7.578E-02	3.036	0.000E+00	0.000	0.000E+00
-7.919	4.811E+03	1.570	4.250E-02	2.950	0.000E+00	0.000	0.000E+00
-7.686	9.682E+03	1.570	9.348E-02	0.160	0.000E+00	0.000	0.000E+00
-7.452	4.874E+03	1.570	1.274E-01	0.050	0.000E+00	0.000	0.000E+00
-7.296	4.898E+03	1.570	1.468E-01	0.038	0.000E+00	0.000	0.000E+00
-7.141	4.923E+03	1.570	1.192E-01	0.041	0.000E+00	0.000	0.000E+00
-6.907	9.928E+03	1.570	2.664E-02	0.321	0.000E+00	0.000	0.000E+00
-6.674	5.009E+03	1.570	7.784E-02	3.088	0.000E+00	0.000	0.000E+00
-6.518	5.041E+03	1.570	7.037E-02	3.074	0.000E+00	0.000	0.000E+00
-6.284	1.019E+04	1.570	2.239E-01	0.058	0.000E+00	0.000	0.000E+00
-6.051	5.149E+03	1.570	3.821E-01	0.022	0.000E+00	0.000	0.000E+00
-5.895	5.190E+03	1.570	5.150E-01	0.017	0.000E+00	0.000	0.000E+00
-5.739	5.232E+03	1.570	5.354E-01	0.015	0.000E+00	0.000	0.000E+00
-5.506	1.060E+04	1.570	5.615E-01	0.013	0.000E+00	0.000	0.000E+00
-5.272	5.371E+03	1.570	1.939E-01	0.007	0.000E+00	0.000	0.000E+00
-5.117	5.417E+03	1.570	7.234E-01	0.008	0.000E+00	0.000	0.000E+00
-4.917	8.744E+03	1.570	3.279E+00	0.010	1.899E+05	0.002	7.233E+04
-4.696	8.661E+03	1.570	1.528E+00	0.007	4.844E+05	0.002	1.788E+05
-4.502	1.101E+04	1.570	5.915E-01	0.011	5.767E+05	0.002	2.036E+05
-4.302	1.516E+04	1.570	5.469E-01	0.006	7.357E+05	0.002	2.472E+05
-4.100	1.729E+04	1.570	8.758E-01	0.017	7.739E+05	0.002	2.465E+05
-3.894	2.203E+04	1.570	1.078E+00	-3.111	0.000E+00	0.000	0.000E+00
-3.684	2.124E+04	1.570	3.734E-01	-0.004	0.000E+00	0.000	0.000E+00
-3.500	1.755E+04	1.570	4.566E-01	-3.054	0.000E+00	0.000	0.000E+00
-3.326	1.996E+04	1.570	6.166E-02	-2.884	0.000E+00	0.000	0.000E+00
-3.133	2.208E+04	1.570	5.286E-01	0.030	0.000E+00	0.000	0.000E+00

Z Slice center	Fx (hydrodynamic pressure)		Fy (hydrodynamic pressure)		Fz (hydrodynamic pressure)		Fz_hs (static pressure)
(m)	Mod (N)	Phase (rad)	Mod (N)	Phase (rad)	Mod (N)	Phase (rad)	(N)
-2.925	2.389E+04	1.570	4.386E-01	0.014	0.000E+00	0.000	0.000E+00
-2.704	2.537E+04	1.570	7.601E-02	-2.774	0.000E+00	0.000	0.000E+00
-2.475	2.650E+04	1.570	2.391E-01	-2.996	0.000E+00	0.000	0.000E+00
-2.299	1.356E+04	1.570	7.758E-03	-1.475	0.000E+00	0.000	0.000E+00
-2.120	2.753E+04	1.570	3.547E-01	0.026	0.000E+00	0.000	0.000E+00
-1.880	2.775E+04	1.570	5.726E-01	0.037	0.000E+00	0.000	0.000E+00
-1.701	1.384E+04	1.570	2.456E-01	0.021	0.000E+00	0.000	0.000E+00
-1.525	2.736E+04	1.570	3.014E-01	-0.025	0.000E+00	0.000	0.000E+00
-1.296	2.662E+04	1.570	1.224E-01	-0.184	0.000E+00	0.000	0.000E+00
-1.075	2.548E+04	1.570	7.052E-02	-0.284	0.000E+00	0.000	0.000E+00
-0.867	2.395E+04	1.570	7.576E-02	-0.047	0.000E+00	0.000	0.000E+00
-0.674	2.203E+04	1.570	5.378E-02	0.285	0.000E+00	0.000	0.000E+00
-0.500	1.971E+04	1.570	5.056E-02	2.846	0.000E+00	0.000	0.000E+00
-0.316	2.436E+04	1.570	3.708E-01	-3.041	0.000E+00	0.000	0.000E+00
-0.107	2.612E+04	1.570	3.792E-01	-3.077	0.000E+00	0.000	0.000E+00

TABLE C-3 RAW RESULTS - WAVE LOADS IN 100-YR STORM - 12 M DIAMETER OWC SPAR BUOY

Z Slice center	Fx (hydrodynamic pressure)		Fy (hydrodynamic pressure)		Fz (hydrodynamic pressure)		Fz_hs (static pressure)
(m)	Mod (N)	Phase (rad)	Mod (N)	Phase (rad)	Mod (N)	Phase (rad)	(N)
-35.749	6.729E+04	1.568	4.230E-01	-3.122	6.768E+06	0.009	2.597E+07
-35.226	1.272E+05	1.568	8.651E-01	-0.188	1.904E+06	0.009	7.150E+06
-34.679	1.529E+05	1.568	1.688E+00	3.016	4.500E+05	0.009	1.660E+06
-34.153	1.242E+05	1.568	1.800E+00	0.052	0.000E+00	0.000	0.000E+00
-33.606	1.945E+05	1.568	8.984E+00	-3.085	8.556E+05	-3.133	-2.988E+06
-33.076	1.934E+05	1.568	8.246E+00	0.131	8.326E+05	-3.133	-2.835E+06
-32.574	9.159E+04	1.568	1.235E+00	3.110	4.074E+05	-3.133	-1.361E+06
-32.002	1.840E+05	1.569	9.467E+00	-3.087	7.967E+05	-3.133	-2.612E+06
-31.472	1.774E+05	1.568	7.775E+00	-3.114	7.723E+05	-3.133	-2.468E+06
-30.979	8.424E+04	1.568	3.427E+00	3.083	3.768E+05	-3.133	-1.181E+06
-30.465	1.649E+05	1.568	7.482E-01	2.653	7.349E+05	-3.133	-2.259E+06
-29.949	1.557E+05	1.568	4.677E+00	-0.005	5.471E+05	-3.133	-1.601E+06
-29.383	1.464E+05	1.568	1.565E+00	-0.137	4.469E+05	-3.133	-1.242E+06
-28.844	6.940E+04	1.568	2.470E+00	-3.081	1.033E+05	-3.133	-2.364E+05
-28.325	1.326E+05	1.568	1.169E+01	3.120	4.240E+05	-3.133	-1.130E+06
-27.761	1.232E+05	1.568	9.884E+00	3.112	4.056E+05	-3.133	-1.045E+06
-27.224	5.800E+04	1.568	6.591E-01	-0.080	9.444E+04	-3.133	-1.961E+05
-26.684	1.094E+05	1.568	1.287E+01	-0.015	3.814E+05	-3.133	-9.414E+05
-26.117	1.002E+05	1.568	3.715E+00	-0.080	3.622E+05	-3.133	-8.633E+05
-25.657	4.672E+04	1.568	1.042E+01	-3.138	1.438E+05	-3.133	-3.209E+05
-25.197	8.681E+04	1.568	1.835E+01	3.114	3.342E+05	-3.133	-7.569E+05
-24.626	6.673E+04	1.568	1.026E+01	-0.029	4.121E+05	-3.133	-9.313E+05
-24.082	5.437E+04	1.568	2.100E+00	-3.102	5.927E+05	-3.133	-1.357E+06
-23.556	5.204E+04	1.568	2.464E+00	-3.094	5.965E+05	-3.133	-1.330E+06
-23.025	3.175E+04	1.568	7.444E-01	-2.613	3.781E+05	-3.133	-8.237E+05
-22.568	4.051E+04	1.568	1.523E+01	-3.131	0.000E+00	0.000	0.000E+00
-22.100	3.993E+04	1.568	8.854E+00	-0.008	0.000E+00	0.000	0.000E+00
-21.572	3.951E+04	1.568	1.444E+01	-0.002	0.000E+00	0.000	0.000E+00
-21.045	3.922E+04	1.568	8.735E+00	-0.001	0.000E+00	0.000	0.000E+00
-20.518	3.903E+04	1.568	1.086E+00	-3.129	0.000E+00	0.000	0.000E+00
-19.991	3.892E+04	1.568	8.004E+00	-3.140	0.000E+00	0.000	0.000E+00
-19.463	3.887E+04	1.568	9.382E+00	-3.140	0.000E+00	0.000	0.000E+00
-18.936	3.888E+04	1.568	6.947E+00	-3.141	0.000E+00	0.000	0.000E+00
-18.409	3.894E+04	1.568	2.608E+00	3.141	0.000E+00	0.000	0.000E+00
-17.882	3.904E+04	1.568	1.710E+00	0.005	0.000E+00	0.000	0.000E+00
-17.354	3.917E+04	1.568	4.158E+00	0.004	0.000E+00	0.000	0.000E+00
-16.827	3.934E+04	1.568	4.217E+00	0.004	0.000E+00	0.000	0.000E+00

Z Slice center	Fx (hydrodynamic pressure)		Fy (hydrodynamic pressure)		Fz (hydrodynamic pressure)		Fz_hs (static pressure)
-16.300	3.955E+04	1.568	2.727E+00	0.007	0.000E+00	0.000	0.000E+00
-15.773	3.978E+04	1.568	5.586E-01	0.036	0.000E+00	0.000	0.000E+00
-15.246	4.004E+04	1.568	1.388E+00	3.127	0.000E+00	0.000	0.000E+00
-14.718	4.034E+04	1.568	2.257E+00	3.132	0.000E+00	0.000	0.000E+00
-14.191	4.066E+04	1.568	1.882E+00	3.130	0.000E+00	0.000	0.000E+00
-13.664	4.102E+04	1.568	7.661E-01	3.112	0.000E+00	0.000	0.000E+00
-13.137	4.142E+04	1.568	5.553E-01	0.048	0.000E+00	0.000	0.000E+00
-12.609	4.185E+04	1.568	1.542E+00	0.021	0.000E+00	0.000	0.000E+00
-12.082	4.232E+04	1.568	1.674E+00	0.025	0.000E+00	0.000	0.000E+00
-11.555	4.284E+04	1.568	9.432E-01	0.056	0.000E+00	0.000	0.000E+00
-11.028	4.340E+04	1.568	1.795E-01	2.791	0.000E+00	0.000	0.000E+00
-10.500	4.402E+04	1.568	1.154E+00	3.083	0.000E+00	0.000	0.000E+00
-9.973	4.471E+04	1.568	1.496E+00	3.098	0.000E+00	0.000	0.000E+00
-9.446	4.546E+04	1.568	7.244E-01	3.068	0.000E+00	0.000	0.000E+00
-8.919	4.628E+04	1.568	8.296E-01	0.047	0.000E+00	0.000	0.000E+00
-8.391	4.717E+04	1.568	2.025E+00	0.018	0.000E+00	0.000	0.000E+00
-7.864	4.811E+04	1.568	1.696E+00	0.034	0.000E+00	0.000	0.000E+00
-7.233	7.018E+04	1.569	7.579E-01	2.915	7.090E+05	0.009	4.093E+05
-6.589	7.573E+04	1.568	6.418E-01	0.107	2.379E+06	0.009	1.292E+06
-6.037	1.118E+05	1.568	1.097E+00	3.052	3.102E+06	0.009	1.533E+06
-5.518	1.346E+05	1.568	6.404E+00	-3.125	3.324E+06	0.009	1.489E+06
-5.014	1.925E+05	1.568	4.739E+00	0.097	2.166E+06	0.009	8.951E+05
-4.435	2.530E+05	1.568	6.993E+00	-0.069	0.000E+00	0.000	0.000E+00
-3.910	1.723E+05	1.568	2.333E-01	0.648	0.000E+00	0.000	0.000E+00
-3.470	1.944E+05	1.568	2.191E+00	2.967	0.000E+00	0.000	0.000E+00
-2.869	3.170E+05	1.568	5.177E-01	-0.022	0.000E+00	0.000	0.000E+00
-2.252	2.168E+05	1.568	2.011E+00	-0.081	0.000E+00	0.000	0.000E+00
-1.765	2.116E+05	1.568	5.206E-01	0.321	0.000E+00	0.000	0.000E+00
-1.304	1.979E+05	1.568	4.967E-01	2.352	0.000E+00	0.000	0.000E+00
-0.542	4.937E+05	1.568	3.852E-01	2.959	0.000E+00	0.000	0.000E+00